



VirginiaTech
Invent the Future

**VIRGINIA POLYTECHNIC INSTITUTE
AND STATE UNIVERSITY**

The Charles E. Via, Jr. Department
of Civil and Environmental Engineering
Blacksburg, VA 24061

Structural Engineering and Materials

**EVALUATION OF THE EFFECT OF BOAT-SHAPED WELDS AND
PNEUMATIC POWER ACTUATED FASTENERS
ON THE SEISMIC BEHAVIOR OF MOMENT FRAMES**

By

**Steven H. Florig
Graduate Research Assistant**

**Matthew R. Eatherton, Ph.D., S.E.
Assistant Professor**

December 2015

EXECUTIVE SUMMARY

The study described in this report evaluates how three types of artifacts (boat-shaped weld repairs and two sizes of pneumatically applied power actuated fasteners) might affect the low cycle fatigue performance of steel special moment resisting frames (SMRF) if they were applied in the protected zone (e.g. plastic hinge region of the beams). To evaluate the effect of artifacts on low cycle fatigue behavior, a series of monotonic tension coupon tests, and cyclic bend coupon tests were conducted and the results compared to companion full-scale moment connection tests and companion coupon tests previously conducted on specimens with no artifacts and with artifacts shown to have acceptable low cycle fatigue performance in full-scale tests.

Bend tests consist of flat plate coupons cut from the flange of wide flange beams that are cyclically bent around two opposing rollers (a diameter of 11 in. was used in this study) imposing fully reversed deformation cycles with constant amplitude peak strain gradient. During the bend tests, several video cameras monitor and record the condition of the faces of the specimen to visually determine the cycle in which fracture initiation and full section fracture occur. Monotonic tension tests are similarly conducted on flat plate coupons.

A total of twenty-four cyclic bend tests and monotonic axial tension tests were conducted on specimens cut from W24x62 and W36x150 beams used in the companion full-scale testing program. Specimen dimensions were selected to have a width to thickness aspect ratio of 5:1. The three artifacts investigated in this study included 0.199 in. x 0.625 in. long pneumatic actuated fasteners, 0.199 in. x 0.75 in. pneumatic actuated fasteners, and boat-shaped weld repairs. The performance of these artifacts was compared to the results of identical tests on powder actuated fasteners, and bare steel control specimens tested in a companion study. The steel used for these tests was cut from the same flange material as in the companion study.

The results of these tests are used to evaluate whether a moment connection with an artifact applied in the protected zone would be expected to satisfy qualification standards in the AISC Seismic Provisions. This is done by demonstrating equivalent or better low cycle fatigue resistance as compared to artifacts already shown to satisfy SMRF qualification. If an artifact is shown to

have similar or less effect on fracture resistance (measured by monotonic elongation at fracture, cycles to fracture initiation, and cycles to full fracture in bend tests) as compared to an artifact already shown acceptable through full-scale testing, then by equivalence it too would be expected to satisfy SMRF qualification. The current test results are therefore compared to previous tests on specimens with powder actuated fasteners which serve as benchmark artifacts because full-scale moment connection tests with those artifacts satisfied SMRF qualification in a companion study.

It was found that these three artifacts had a significant effect on the number of cycles required for fracture initiation and failure as compared to the bare steel specimens. It was also found that none of the artifacts tested here performed quite as well as the powder actuated fasteners. The average number of cycles to fracture initiation were 5.3, 2.5, 2.5, 2.3, and 1.2 for the bare steel, powder actuated fasteners, 5/8" pneumatic actuated fasteners, 3/4" pneumatic actuated fasteners, and boat shaped weld repairs respectively. The average number of cycles to final fracture were 8.6, 6.4, 4.8, 4.0, and 4.3 for the bare steel, powder actuated fasteners, 5/8" pneumatic actuated fasteners, 3/4" pneumatic actuated fasteners, and boat shaped weld repairs respectively.

Based on the results of the monotonic and cyclic tests conducted on boat-shaped weld repairs and pneumatic power actuated fasteners, the following conclusions were made:

- The 0.199 in. x 0.625 in. pneumatic PAF produced monotonic elongation and number of cycles to fracture initiation and final fracture that were similar or slightly less than benchmark specimens containing powder actuated fasteners. It is not possible, therefore, to conclude that these artifacts are acceptable (acceptable defined as likely to satisfy SMRF qualification criteria based on demonstrating equivalence) in the protected zone of special moment resisting frames. However, since the results were not substantially less, it is possible that these artifacts applied in the protected zone would not cause significant fracture before SMRF qualification. To be sure, it would be necessary to conduct full scale moment connection tests to verify.
- The 0.199 in. x 0.75 in. long pneumatic PAF produced even lower monotonic elongation and cycles to fracture. For the thinner material (0.59" thick flange material included in this testing program), the fastener passed all the way through

the material and seemed to negatively affect the low cycle fatigue performance. For power (powder or pneumatic) actuated fasteners, it is advisable to limit the length of the fastener to be less than the thickness of the material.

- The boat-shaped weld repair specimens developed fracture earlier than the pneumatic or powder actuated fastener specimens. More research is required to develop methods to repair defects in the protected zone that don't have such large impact on low cycle fatigue resistance. Some additional boat shaped weld repair specimens are being tested with smaller wire GMAW welding rather than the large diameter wire FCAW welding conducted in this study.

ACKNOWLEDGEMENTS

This material is based on work supported by the American Institute of Steel Construction and Pneutek. The authors appreciate the input from AISC and especially Tom Schlafly and Duane Miller. Valuable assistance in the preparation and conducting of tests was provided by Patrick O'Brien as well as lab technicians Dennis Huffman and Brett Farmer.

TABLE OF CONTENTS

Contents

EXECUTIVE SUMMARY	i
ACKNOWLEDGEMENTS	iii
TABLE OF CONTENTS	iv
CHAPTER 1 INTRODUCTION	6
1.1 Overview	6
1.2 Scope of Artifacts Investigated	7
1.3 Organization of This Report.....	8
CHAPTER 2 EXPERIMENTAL TESTING PROGRAM.....	9
2.1 Introduction	9
2.3 Overview of Testing Approach with Flat Plate Specimens	9
2.4 Monotonic Uniaxial Tension Tests	9
2.5 Cyclic Bend Tests.....	10
2.6 Specimen Preparation with Artifacts.....	14
2.6.1 Pneumatic Actuated Fasteners (PnAF).....	14
2.6.5. Boat Shaped Weld Repair (BSWR).....	16
CHAPTER 3 TEST RESULTS.....	20
3.1 Introduction	20
3.2 Monotonic Axial Tests	20
3.3 Cyclic Bend Test Results	23
CHAPTER 4 SUMMARY, CONCLUSIONS, AND FURTHER RESEARCH NEEDS	35
REFERENCES.....	38
APPENDIX A DESCRIPTION OF BEND TEST FRACTURES	40

A.1 5/8” Pneumatic Actuated Fasteners (PnAF)	40
A.2 3/4” Pneumatic Actuated Fasteners (PnAF)	45
A.3 Boat Shaped Weld Repair (BSWR).....	51

CHAPTER 1 INTRODUCTION

1.1 Overview

After the 1994 Northridge Earthquake and the 1995 Kobe Earthquake, unexpected fractures were observed in steel beam-to-column moment-resisting connections. This led to many experimental programs focused on a range of topics including reduced beam section connections (e.g. Chi and Uang 2002), extended end plate connections (e.g. Adey et al. 2000), effect of composite slabs (e.g. Hajjar et al. 1998), panel zone strength (e.g. Lee et al. 2005) and more. A subset of these testing programs included a composite slab with welded shear studs attached to the beam in the plastic hinge region causing geometric and material discontinuities (e.g. Chi and Uang 2002, Hajjar et al. 1998, Ricles et al. 2002). One of the beam-to-column connection specimens with welded shear studs in the plastic hinge region experienced fracture of the flange initiating at the shear stud (Ricles et al. 2002). It was concluded that the fracture of the beam flange was a direct result of the reduced notch toughness of the base metal caused by shear stud welding.

The AISC Seismic Provisions for Structural Steel Buildings (AISC 2010a) define the locations where large inelastic strains are expected to occur as protected zones in which welded, bolted, screwed or shot-in attachments are not allowed. However, during construction, structural steel components erected in real buildings are subjected to a wide range of artifacts including, but not limited to: notches, nicks, welds, powder actuated fasteners, and self-drilling screws. In this report, the word artifact is used to describe discontinuities in the steel due to defects, fasteners, or repairs intended to mitigate defects. Few tests have been conducted on moment resisting connections with these types of artifacts. Full-scale testing of moment resisting connections is expensive which makes it economically infeasible to experimentally examine the wide range of possible structural configurations, artifact types, and artifact locations.

In Eatherton and Abbas (2014), a method was developed for evaluating the acceptance of artifacts in special moment resisting frames (SMRF) using the results of relatively economical coupon tests. This method consists of conducting monotonic and cyclic coupon tests and demonstrating that the artifact under consideration demonstrates equivalent or better behavior than benchmark artifacts that have been shown in full-scale testing to satisfy SMRF qualification

criteria. The process for evaluating fracture resistance using this method can be found detailed in Eatherton and Abbas (2014).

Multiple types of artifacts were previously examined using cyclic and monotonic coupon tests to determine fracture resistance in Eatherton and Abbas (2014). These artifacts include powder actuated fasteners, puddle welds, ground filled welds, notch ground to taper, and notch welded and ground smooth. In order to determine whether the current artifacts would likely meet the SMRF qualifications, their results will be compared to the results of bare steel and the powder actuated fastener specimens from Eatherton and Abbas (2014). The powder actuated fasteners were chosen because they were shown to meet the SMRF qualifications in a full scale moment frame test from Eatherton et al. 2013 and in order to demonstrate equivalence, the testing results must be compared to results from an artifact run through the same tests which is already known to meet the SMRF qualifications. If the results from the tested artifacts are shown to have a fracture resistance that is greater than or equal to the artifact that meets SMRF qualifications (in this case, the powder actuated fasteners), then it is demonstrated by equivalence that the tested artifact is likely to also meet SMRF qualifications.

1.2 Scope of Artifacts Investigated

A total of twenty-four cyclic bend tests and monotonic axial tests, were conducted at the Thomas M. Murray Structural Engineering Laboratory at Virginia Tech. The specimens were cut from W24x62 and W36x150 beams used in full-scale SMRF moment connection tests (Eatherton et al. 2013). Three types of specimens were tested including 0.199 in. x 0.625 in. pneumatic actuated fasteners, 0.199 in. x 0.75 in. pneumatic actuated fasteners, and boat shaped weld repairs. Pneumatic actuated fasteners are used in deck attachments that may occur in the plastic hinge region of a SMRF connection. These types of fasteners are also used in the connection of nonstructural elements such as partition walls, pipe racks, and ductwork to the structural steel. The boat shaped weld repairs are a type of weld repair conceived for these tests which could potentially be used for repairing notches, nicks, and gouges in the protected zone of seismic resisting structural systems. No previous testing data exists as to how these repair methods affect the low cycle fatigue resistance of steel sections.

For the coupon bend tests, the coupons were cyclically bent around a roller with a diameter of 11 in. causing cycles with constant amplitude peak strain gradient. Specimen dimensions were selected to have an aspect ratio of 1:5 with respect to the thickness and width. Therefore, the coupons cut from the flanges of W24x62 sections were 0.59 in. thick x 2.95 in. wide and the coupons cut from W36x150 flanges were 0.94 in. thick x 4.7 in. wide. The results from the tests were compared to those from bare steel and powder actuated fasteners (Abbas and Eatherton 2014.)

1.3 Organization of This Report

This report describes relevant background, details of the testing procedures for the different types of artifacts, results from the tests, and a summary of the findings including additional future research needs. The report is organized into the following chapters:

- Chapter 1 describes the motivation for and an introduction to the proposed testing plan for investigating the effect of artifacts on seismic behavior of moment connections using low cycle fatigue loading. It also summarizes what is included in this document.
- Chapter 2 discusses the testing program consisting of cyclic bend tests, and uniaxial monotonic tests. Information is included such as goals of the testing, test matrix, and dimensions and details of the test setup and specimens.
- Chapter 3 presents the results from all the tests conducted.
- Chapter 4 includes a summary of the work and conclusions reached in this study. These include overall observations and recommendations for future work.
- Appendices provide a description of the fracture initiation and propagation throughout each cyclic bend test specimen.

CHAPTER 2 EXPERIMENTAL TESTING PROGRAM

2.1 Introduction

This chapter will present the testing program. The parts of the experimental program that will be discussed are the monotonic uniaxial tension tests on flat plates, and the cyclic bend tests on flat plates. Then, the detailed procedures for implementing each artifact are described.

2.2 Overview of Testing Approach with Flat Plate Specimens

To stay consistent with Eatherton and Abbas (2014), tests on flat plate coupons that represent the web or flange of steel wide flange sections were selected. If fracture occurs in a steel component away from a connection, it typically occurs at the location of a buckle such as the buckling and creasing of HSS braces in concentrically braced frames, or local buckles in a moment frame plastic hinge region. In these cases, fracture occurs in portions of steel plate subjected to a steep strain gradient associated with bending. A cyclic bend test setup using flat plate material was therefore chosen (Eatherton and Abbas 2014).

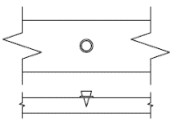
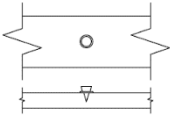
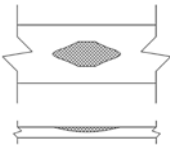
It is the intent of these tests to replicate those done previously on bare steel and powder actuated fastener specimens (Eatherton and Abbas 2014). This includes using steel cut from the same flange material as well as using the same test setups and loading protocols. The results can then be compared on a one to one basis to show if the artifacts tested perform as well or better than the powder actuated fasteners shown to meet the SMRF qualifications.

2.3 Monotonic Uniaxial Tension Tests

The specimens were cut from the flanges of beams used in full-scale tests (Eatherton et al. 2013) and small scale cyclic and monotonic tests (Eatherton and Abbas 2014). The specimens were taken from the mid-length of the full-scale beam specimens where no inelastic deformations occurred. The geometry of the coupons and the loading rate for testing was determined as per A370-12a (ASTM 2012) with a total length of 18 in., a gage length of 8 in, and a width of 1.5 in.

A total of 6 monotonic uniaxial tests were conducted with different artifacts to compare to bare steel and powder actuated fastener specimens. Three were cut from the flanges of the W24x62 and the other three were cut from the flanges of the W36x150 specimens. Table 2.1 presents the monotonic uniaxial testing matrix. Results and pictures are presented in the next chapter.

Table 2.1 – Monotonic test matrix.

Artifact Type		Flange Thickness	Artifact Name
1) 5/8" Pneumatic Actuated Fasteners (PnAF)		W24x62 (0.59 in.)	W24-PnAF062.5-Mono-T59
		W36x150 (0.94 in.)	W36-PnAF062.5-Mono-T94
2) 3/4" Pneumatic Actuated Fasteners (PnAF)		W24x62 (0.59 in.)	W24-PnAF075-Mono-T59
		W36x150 (0.94 in.)	W36-PnAF075-Mono-T94
3) Boat Shaped Weld Repair (BSWR)		W24x62 (0.59 in.)	W24-BSWR-Mono-T59
		W36x150 (0.94 in.)	W36-BSWR-Mono-T94

2.4 Cyclic Bend Tests

As shown in Figure 2.1, a plate specimen is cyclically bent around opposing rollers creating a constant peak curvature which implies cycles with constant strain amplitude assuming uniform strain distribution.

Two loading arms are connected to the actuator to hold the two 11 in. diameter rollers as shown in Figure 2.1. The specimen is clamped between the two rollers and moved back and forth. As shown in Figure 2.1(b), Figure 2.1(c), and Figure 2.2, the specimen is forced to bend around the rollers as the specimen is pushed between two guides. The moving parts are shown in green in Figure 2.2(b) and the fixed parts are shown in blue. For the 0.59 in. and 0.94 in. thick specimens,

the calculated strain at the extreme fiber was 0.051 in./in. and 0.079 in./in. respectively, and the calculated radius of curvature was 5.795 in. and 5.97 in. respectively.

The coupon is held in between the two 11 in. diameter rollers and displaced using a loading arm connected to the actuator. A 1 3/8 inch bolt is used to hold the top roller tight against the specimen while accommodating a range of 0.5 to 1.0 in. plates through use of slotted holes in the loading arms. The bolt is designed to be slip critical and thus prevent slippage during loading. To ensure that the specimen was secured between the rollers, a jack was used to apply loading on the top roller while tensioning the 1 3/8 in. bolt. The load applied by the jack was 7 kips. A schematic example of the bending action during one cycle is shown in Figure 2.2.

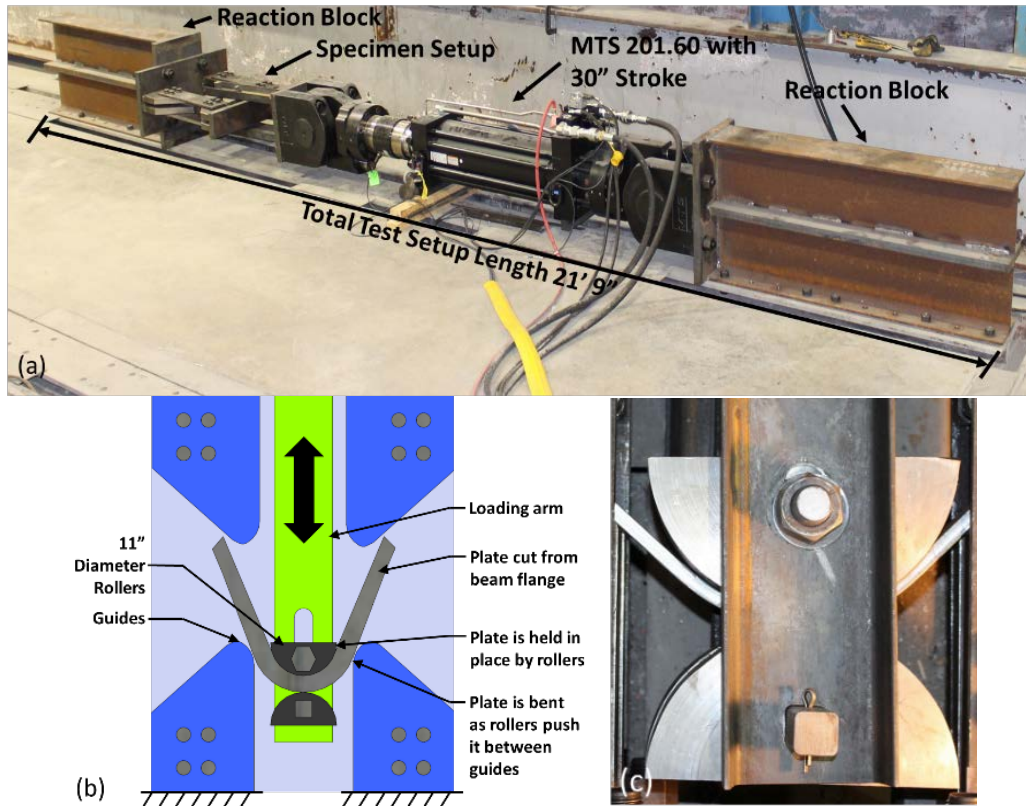


Figure 2.1 (a) Cyclic bend test overall view, (b) top view, and (c) photograph of test setup top view.

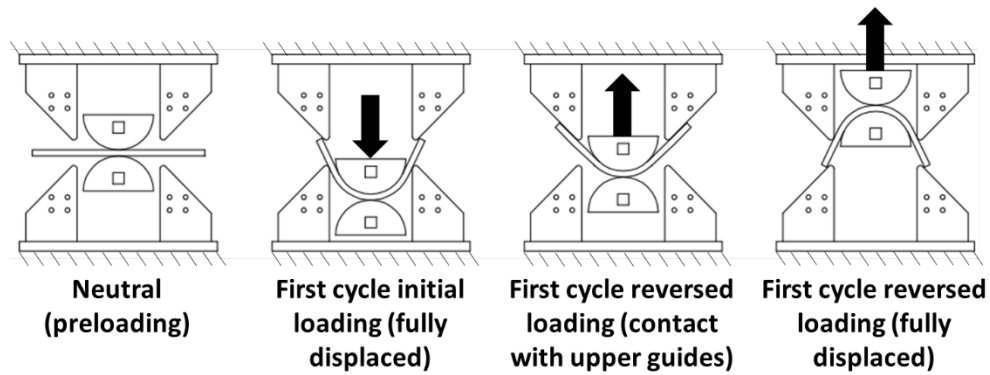


Figure 2.2 – Cyclic bend test bending steps for first cycle.

A total of 18 cyclic bend tests were performed as part of this study, 9 cut from the flanges of W24x62 beams and the other 9 were cut from the flanges of W36x150 beams. The cyclic test matrix can be found in Table 2.2. Specimen dimensions were selected to have an aspect ratio of 1:5 with respect to the thickness and width. Therefore, the coupons cut from the flange of a W24x62 section are 0.59 in. x 2.95 in. and the coupons cut from W36x150 are 0.94 in. x 4.7 in. Three different specimen geometries were tested; an unnotched specimen, a small notch ($R = 0.25$ in.) and a large notch ($R = 1.00$ in.) as shown in Figure 2.4. Notches were used to vary the stress triaxiality and equivalent plastic strain.

The specimens were cycled with a constant displacement protocol between -5 in. and +5 in. using a MTS 201.60 actuator with a stroke length of 30 in. Loading rates for the 0.59 in. and 0.94 in. thick specimens were both 5 in/min. This rate was selected based on trial tests (not reported here) to check the integrity of the test setup and mitigate the possibility of early damage due to rapid loading.

The rollers are split into two parts (front and back pieces) with a 1 in. gap in between as shown in Figure 2.3 (a). Six high definition cameras were mounted in the gap to monitor both faces of the specimens as shown in Figure 2.3 (b). The cameras were used to record the time and location of fracture initiation as well as recording the fracture propagation and full section fracture. The side of the specimen where the artifact was located was considered the top side and was placed towards the top roller.

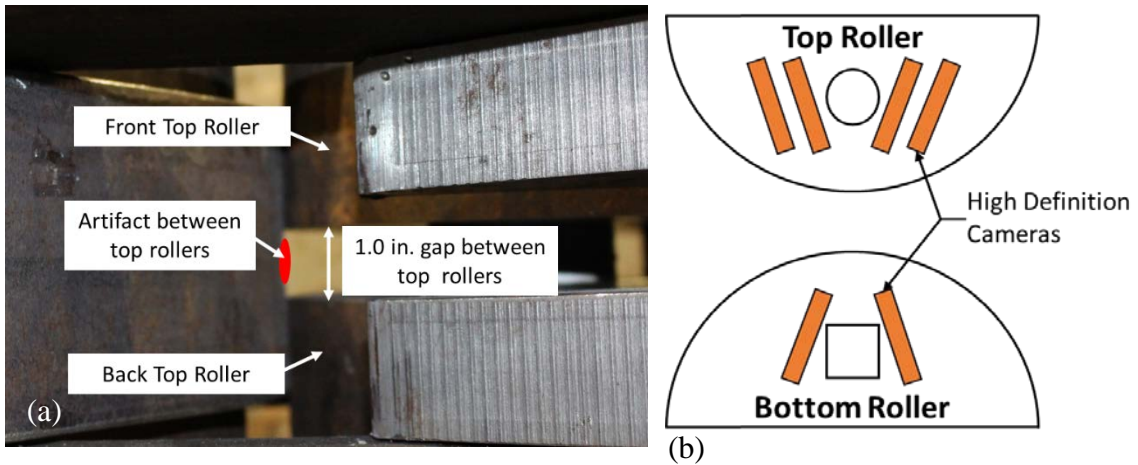


Figure 2.3 – (a) Close up side view of top front and back rollers with 1 in. gap between them, (b) high definition cameras layout on the back top and bottom rollers.

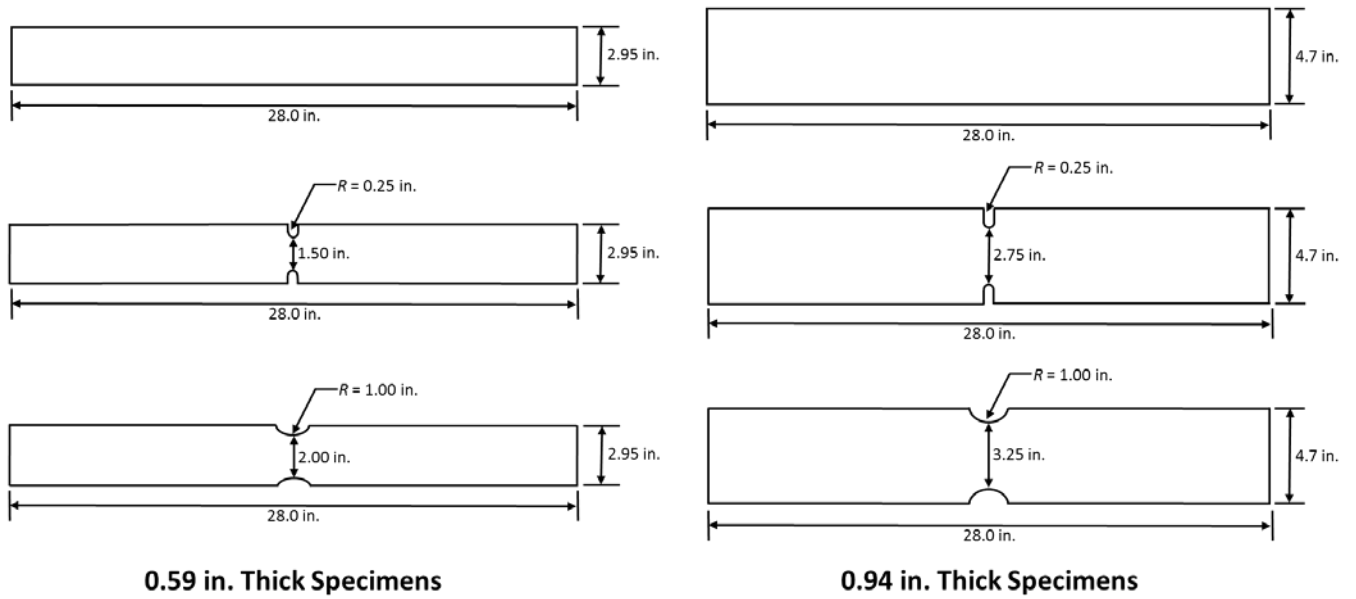
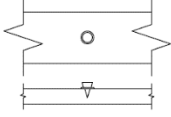
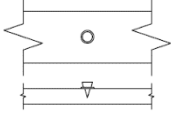
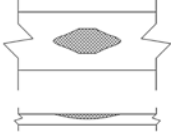


Figure 2.4 – Cyclic bend test specimens for both W24x62 and W36x150.

Table 2.2 – Bend test testing matrix

Artifact Type		Specimen Thickness	Specimen Name	Notched Radius (in.)
1) 0.199 in. x 0.625 in. Pneumatic Actuated Fasteners (PnAF)		W24x62 (0.59 in.)	W24-PnAF062.5-T59-R000	N/A
			W24-PnAF062.5-T59-R025	0.25
			W24-PnAF062.5-T59-R100	1.00
		W36x150 (0.94 in.)	W36-PnAF062.5-T94-R000	N/A
			W36-PnAF062.5-T94-R025	0.25
			W36-PnAF062.5-T94-R100	1.00
2) 0.199 in. x 0.75 in. Pneumatic Actuated Fasteners (PnAF)		W24x62 (0.59 in.)	W24-PnAF075-T59-R000	N/A
			W24-PnAF075-T59-R025	0.25
			W24-PnAF075-T59-R100	1.00
		W36x150 (0.94 in.)	W36-PnAF075-T94-R000	N/A
			W36-PnAF075-T94-R025	0.25
			W36-PnAF075-T94-R100	1.00
3) Boat Shaped Weld Repairs (BSWR)		W24x62 (0.59 in.)	W24-BSW-T59-R000	N/A
			W24-BSW-T59-R025	0.25
			W24-BSW-T59-R100	1.00
		W36x150 (0.94 in.)	W36-BSW-T94-R000	N/A
			W36-BSW-T94-R025	0.25
			W36-BSW-T94-R100	1.00

2.5 Specimen Preparation with Artifacts

Three different artifacts were studied: 0.199 in. x 0.625 in. and 0.199 in. x 0.75 in. Pneumatic Actuated Fasteners (PnAF), and Boat Shaped Weld Repairs (BSWP). The application of each artifact is presented in this section. The BSWP artifacts which required welding were conducted by a certified lab technician with substantial previous welding experience.

2.5.1 Pneumatic Actuated Fasteners (PnAF)

The PnAFs used in this study were Pneutek 0.199 in. x 0.75 in. (K66075) and Pneutek 0.199 in. x 0.625 in. (K66062) steel decking nails. The PnAFs were shot into test specimens with a Pneutek PT-2000Z pneumatic gun. Successful installation of a PnAF is determined by Pneutek's fastener inspection criteria. Simple visual inspection is all that is required to determine if a fastener is properly installed. As shown in Figure 2.5, the fastener must be installed so that there is tight

contact between the fastener head and the steel, or the collation material and the steel. A PnAF has two variables that determine how far the fastener penetrates into the steel. These include the toughness of the steel, and the pressure that the pneumatic gun is set to. In order to ensure the PnAF is installed properly, practice shots were taken on scrap steel of the same type and thickness. The toughness of the steel was found to be relatively constant so only the pressure that the gun was set to affected penetration.

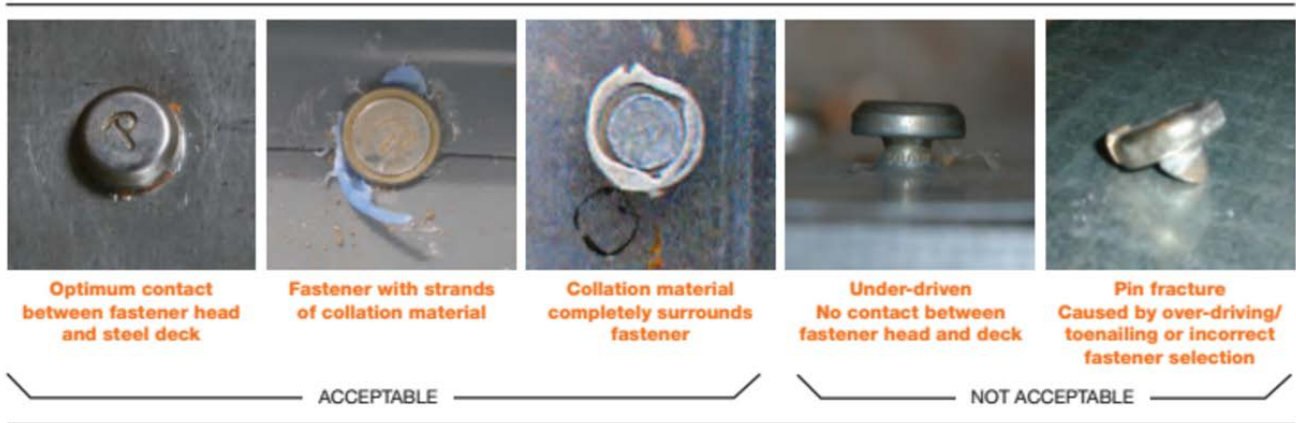


Figure 2.5 – PnAF Visual Inspection Guide for Acceptable Fastener Installation. (From Pneutek’s Fastener Inspection Guide for Steel Decking)

One fastener was shot into the center of each specimen and inspected for proper installation. Many times, the collation material was still on the fastener but was in tight contact with the steel rendering it acceptable. In these cases, the collation material was intentionally cut off so the video cameras in the test setup could have a better view of the area around the head of the fastener. An example of a ready to test specimen can be found in Figure 2.6.



Figure 2.6 – Completed fastener specimen.

2.6.5. Boat Shaped Weld Repair (BSWR)

Repair methods for deeper notches or gouges in the protected zone can be done by filling with weld and grinding smooth. According to AWS D1.8, when gouges and notches are repaired by grinding, the ground area shall provide a gradual taper to the surface of the base metal. In the direction parallel to the member axis, the taper shall not be greater than 1:5. In the direction transverse to the member axis, the taper shall not be greater than 1:2.5. This convention was used to determine the size of the weld repair. Also as per AWS D1.8, following welding, the repair weld shall be ground to a smooth contour with a surface roughness not to exceed 500 μin . The resultant thickness of the repaired area shall be no less than the base metal thickness less 1/16 in.

Each BSWR was created by grinding a 1/4" deep notch into the center of each specimen with a metal grinding wheel, then following AWS D1.8 to create a slope up to the surface of the steel that was within the limits of 1:5 and 1:2.5 along the member axis and perpendicular to the member axis respectively. This resulted in a ground out area that was a minimum of 3.3" long X

1.25" wide X 0.25" deep as shown in Figure 2.7. After the notch was ground out, 5 passes of 1/4" weld beads were used in the bottom of the notch with 2 passes of 1/4" weld beads overtop to fill in the full volume of the notch. Flux Core Arc Welding (FCAW) was used for the BSWR specimens with a 70 ksi wire (Lincoln Electric Innershield NR-203 NiC Self-Shielded Core Wire). Small runoff tabs were placed on either side of the notch during welding to promote good weld material at the repair ends. Once the weld was completed, the runoff tabs were broken off and the weld was ground smooth. A roughness gauge was used to visually inspect the ground weld and determine its roughness. A picture of a completed weld and finished, ground specimen can be found in Figure 2.8. Once the welds were ground smooth, there were occasionally defects present. These defects were ground out with slope not exceeding 1:2.5. The ground defects were finished to the same smoothness as the rest of the weld. Figure 2.9 shows what a typical ground defect looks like.

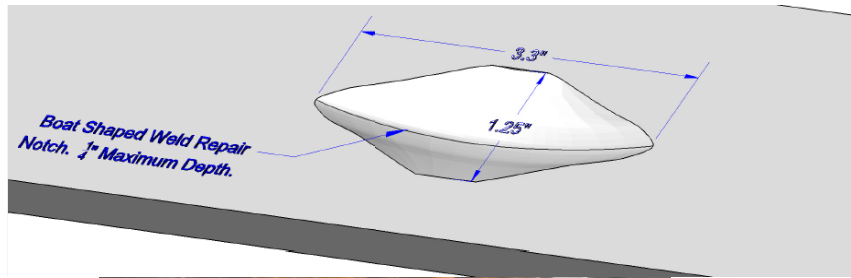


Figure 2.7 – (a) Dimensions of the boat shaped notch, and (b) finished ground notch before welding.

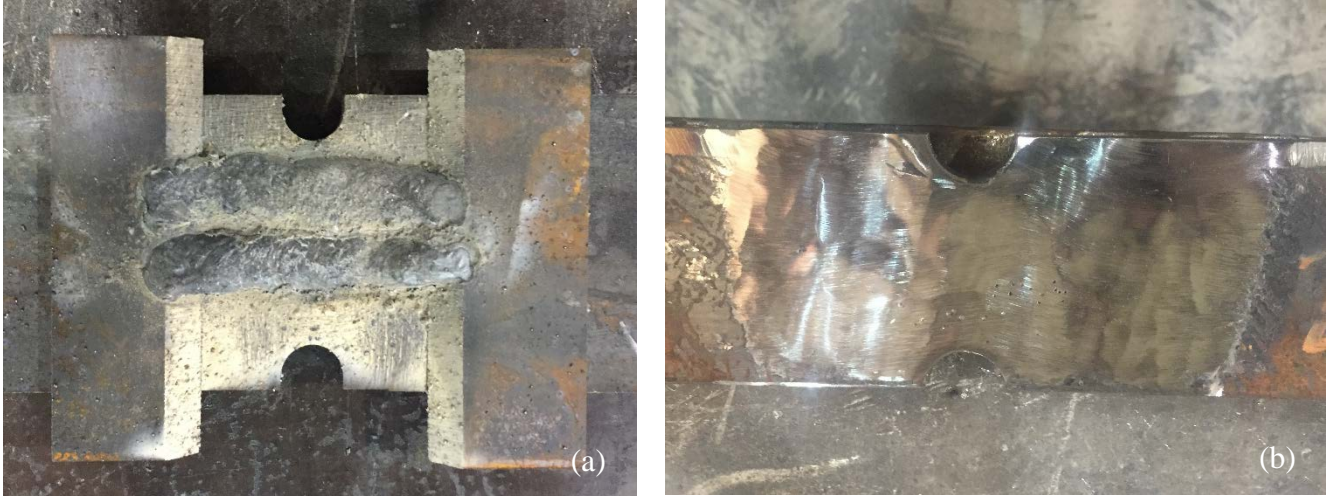


Figure 2.8 – (a) Completed weld showing runoff tabs and (b) finished ground BSWR specimen.

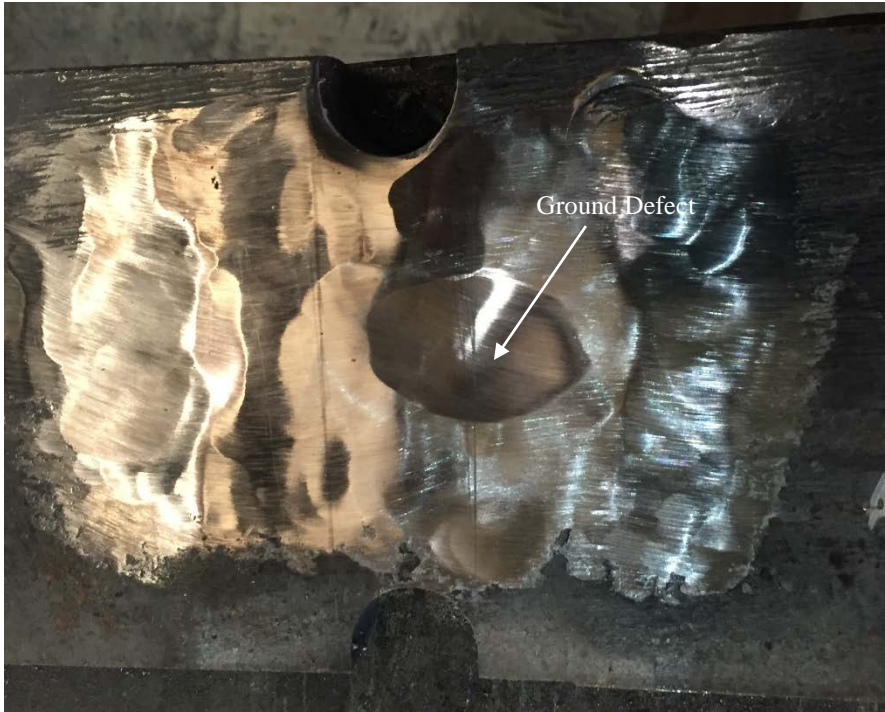


Figure 2.9 – Ground out defect in BSWR specimen.

CHAPTER 3 TEST RESULTS

3.1 Introduction

This chapter presents the results from the testing program. First, the monotonic test results are presented followed by a description of behavior for each bend test specimen. The cyclic bend tests are then summarized with number of cycles to fracture initiation and full fracture.

3.2 Monotonic Axial Tests

A total of 6 monotonic axial tests were conducted with different artifacts to compare to the results from Eatherton and Abbas 2014. Section 2.4 gives details of the test specimens which included 0.59 in. thick specimens cut from W24x62 flanges and 0.94 in. thick specimens cut from W36x150 flanges. Figure 3.1 shows a typical test setup. It was noticed that there was some variability in the measured thickness before testing.

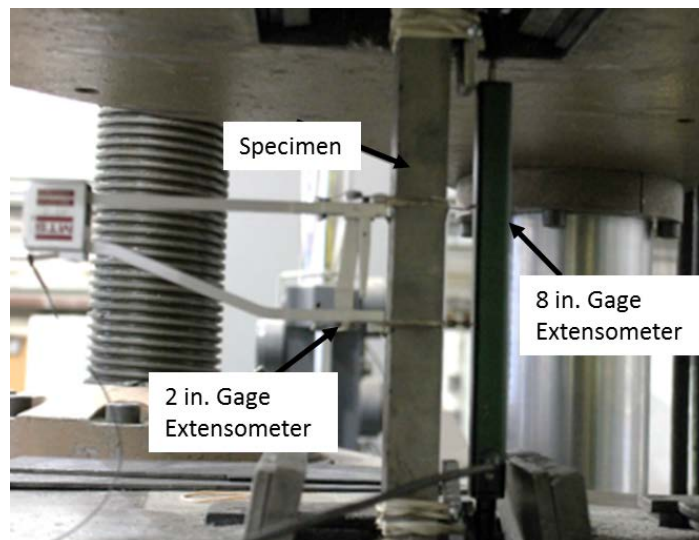


Figure 3.1 – Tensile monotonic test setup with two extensometers mounted one at each side of the specimen.

Figure 3.2 and Figure 3.3 show the load-displacement data for the 0.59 in. thick and 0.94 in. thick specimens with the different artifacts tested and compares them to the results from the bare specimens and the PAF specimens from Ebrahim and Abbas (2014). The six specimens produced yield stresses ranging from 48 to 53 ksi, and ultimate stresses ranging from 61 to 67 ksi.

Detailed yield stress, ultimate stress, and elongation data for each control specimen and tested specimen is presented in Table 3.1. The boat-shaped weld repair specimen was invalid because the specimen was substantially damaged during fabrication.

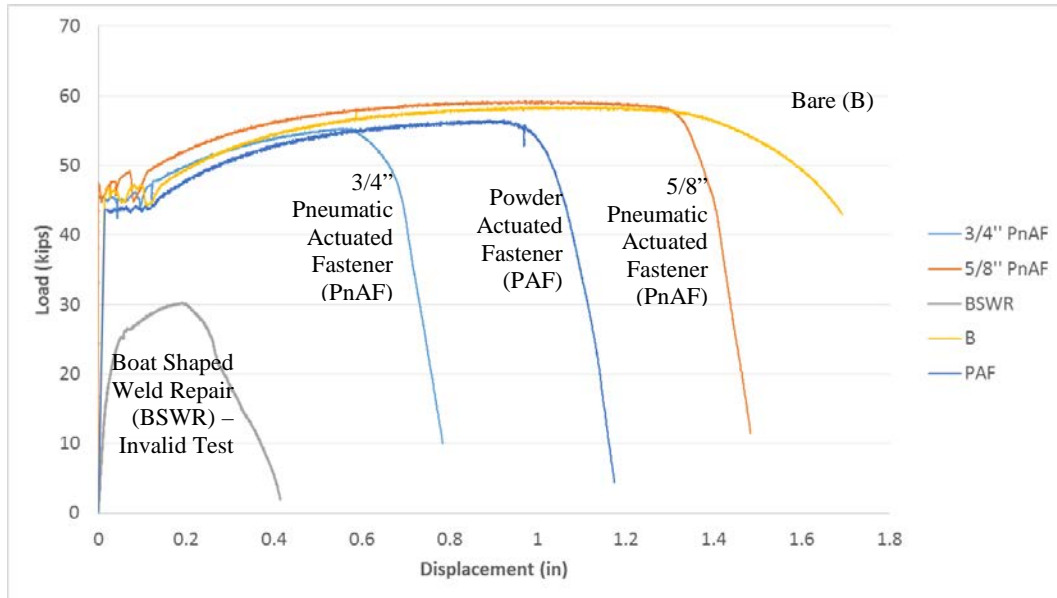


Figure 3.2 – Monotonic 0.59 in. thick tension coupon test data with various artifacts.

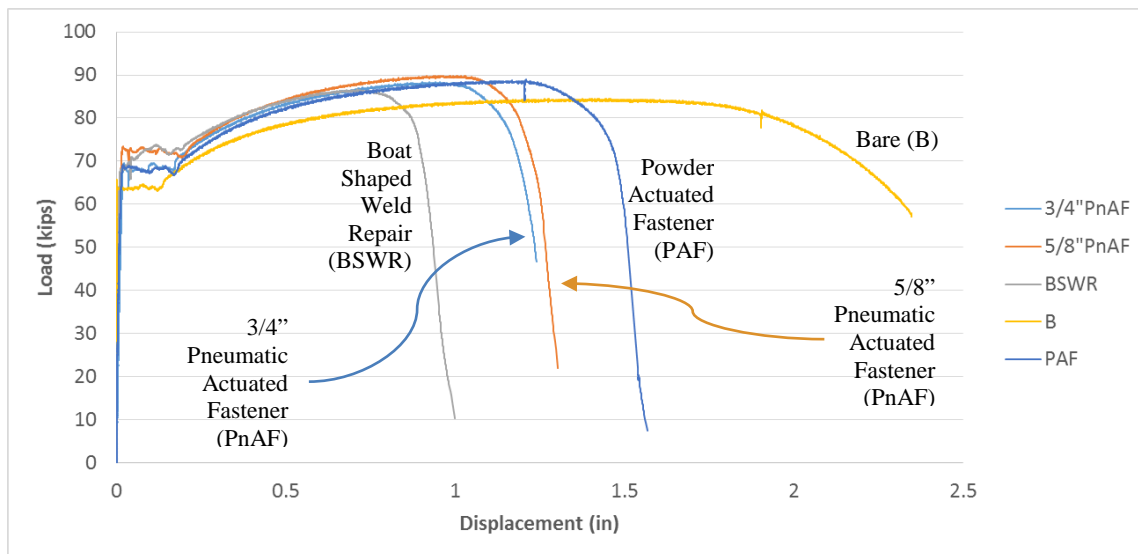
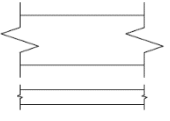
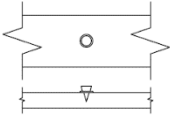
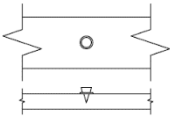
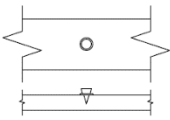
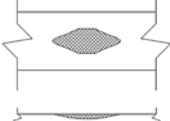


Figure 3.3 – Monotonic 0.94 in. thick tension coupon test data with various artifacts.

The bare specimens had an average elongation at fracture of 25.3% (Eatherton and Abbas 2014). The two powder actuated fastener (PAF) specimens had a percent elongation of 14.7 and 19.6 percent for the 0.59in and 0.94in specimens respectively (Eatherton and Abbas 2014). Comparing these results to the pneumatic actuated fasteners (PnAF's) and the boat shaped weld repairs (BSWR), the average specimen elongation for the two lengths of PnAF's was 98.7 and 82.4 percent of the PAF elongation for the 0.59in and 0.94in specimens respectively. The specimen elongation for the BSWR was 63.7 percent of the PAF elongation for the 0.94in specimen. As can be seen from the data, none of the artifacts performed quite as well as PAF's.

Table 3.1 – Monotonic test results for W24x62 and W36x150 specimens with artifacts.

Artifact Type		Flange Thickness	Artifact Name	F _y (ksi)	F _u (ksi)	Elongation (%)
1) No Artifact (B)		W24x62 (0.59 in.)	W36-B-Mono-T59	51	66	21.2
		W36x150 (0.94 in.)	W36-B-Mono-T94	45	60	29.4
2) Powder Actuated Fasteners (PAF)		W24x62 (0.59 in.)	W24-PAF-Mono-T59	47	64	14.7
		W36x150 (0.94 in.)	W36-PAF-Mono-T94	48	63	19.6
3) 5/8" Pneumatic Actuated Fastener (PnAF)		W24x62 (0.59 in.)	W24-PnAF062.5-Mono-T59	52	67	18.6
		W36x150 (0.94 in.)	W36-PnAF062.5-Mono-T94	52	64	16.3
4) 3/4" Pneumatic Actuated Fastener (PnAF)		W24x62 (0.59 in.)	W24-PnAF075-Mono-T59	51	63	10.4
		W36x150 (0.94 in.)	W36-PnAF075-Mono-T94	48	63	16.0
5) Boat Shaped Weld Repair (BSWR)		W24x62 (0.59 in.)	W24-BSWR-Mono-T59	N/A	N/A	N/A
		W36x150 (0.94 in.)	W36-BSWR-Mono-T94	51	61	12.5

3.3 Cyclic Bend Test Results

Eighteen bend tests were conducted using different artifacts to compare to the control results from the bare steel and PAF artifacts tested in Eatherton and Abbas 2014. Photographs

showing fracture initiation and final fracture for each specimen are included in Appendix A. Results for the cyclic bend tests for the PnAF artifacts and control specimens are summarized in Table 3.2 including the cycle when fracture initiated and the cycle when complete fracture occurred. Results for the cyclic bend tests for the BSWR artifacts are summarized in Table 3.3. The fractures on the BSWR specimens were difficult to identify so the fracture description was broken up into three categories; cycle of first visible defect, fracture initiation cycle (folded steel defect), and final fracture cycle. Pictures of each of these fracture categories can be found in Figures 3.11 and 3.12. The fracture initiation cycle was determined by observing the cycle when the visible defects changed from being very small to what was termed a “folded steel defect”. In nearly every case, the largest fracture propagated from one or multiple folded steel defects which caused the final fracture. It was decided that breaking the BSWR fracture descriptions into three categories would provide a more detailed analysis of how the fractures propagated since there appeared to be three distinct stages of fracture for these specimens. The cycle at which each of the three fracture categories occurred for all BSWR specimens are shown in Table 3.3. Some of the fracture initiation cycle (folded steel defect) cells are labeled N/A which denotes a case where full fracture occurred suddenly before any folded steel defects had the chance to form.

Table 3.2 – Bend test results for control and pneumatic actuated fastener (PnAF) specimens.

Artifact Type	Flange Thickness	Artifact Name	Notched Radius (in.)	Fracture Initiation Cycle	Average Initiation Cycle	Final Fracture Cycle	Average Fracture Cycle
1) No Artifact	0.59 in. (W24x62)	W24-B1-T59-R000	N/A	18	8.3	28	13.3
		W24-B2-T59-R025	0.25	3		5	
		W24-B3-T59-R100	1.00	4		7	
	0.94 in. (W36x150)	W36-B1-T94-R000	N/A	4	2.3	7	4.0
		W36-B2-T94-R025	0.25	1		2	
		W36-B3-T94-R100	1.00	2		3	
2) Powder Actuated Fasteners (PAF)	0.59 in. (W24x62)	W24-PAF1-T59-R000	N/A	3	2.3	18	9.0
		W24-PAF2-T59-R025	0.25	2		4	
		W24-PAF3-T59-R100	1.00	3		5	
	0.94 in. (W36x150)	W36-PAF1-T94-R000	N/A	4	2.7	6	3.7
		W36-PAF2-T94-R025	0.25	2		2	
		W36-PAF3-T94-R100	1.00	2		3	
3) 5/8" Pneumatic Actuated Fasteners (PnAF)	0.59 in. (W24x62)	W24-PnAF062.5-T59-R000	N/A	3	2.7	13	6.3
		W24-PnAF062.5-T59-R025	0.25	2		2	
		W24-PnAF062.5-T59-R100	1.00	3		4	
	0.94 in. (W36x150)	W36-PnAF062.5-T94-R000	N/A	3	2.3	5	3.3
		W36-PnAF062.5-T94-R025	0.25	2		2	
		W36-PnAF062.5-T94-R100	1.00	2		3	
4) 3/4" Pneumatic Actuated Fasteners (PnAF)	0.59 in. (W24x62)	W24-PnAF075-T59-R000	N/A	4	2.7	9	5.0
		W24-PnAF075-T59-R025	0.25	2		2	
		W24-PnAF075-T59-R100	1.00	2		4	
	0.94 in. (W36x150)	W36-PnAF075-T94-R000	N/A	2	2.0	5	3.0
		W36-PnAF075-T94-R025	0.25	2		2	
		W36-PnAF075-T94-R100	1.00	2		2	

Table 3.3-Bend test results for boat shaped weld repair specimens (BSWR)

Artifact Type	Flange Thickness	Artifact Name	Notched Radius (in.)	Cycle of First Visible Defect	Average Cycle of First Visible Defect	Fracture Initiation Cycle (Folded Steel Defect)	Average Initiation Cycle	Final Fracture Cycle	Average Fracture Cycle
3.3" X 1.25" X 0.25" Boat Shaped Weld Repair	0.59" (W24X62)	W24-BSW-T59-R000	N/A	1	1.3	2	2.0	13	6.0
		W24-BSW-T59-R025	0.25	2		N/A		2	
		W24-BSW-T59-R100	1.00	1		2		3	
	0.94" (W36X150)	W36-BSW-T94-R000	N/A	1	1.0	2	2.0	4	2.7
		W36-BSW-T94-R025	0.25	1		N/A		2	
		W36-BSW-T94-R100	1.00	1		2		2	

The following excerpt describing the fracture initiation and propagation of the bare steel specimens and the power actuated fastener specimens was taken directly from Eatherton and

Abbas, 2014. These descriptions will be used for comparison with the test results from the artifacts tested here.

Bare Specimens (B)

Bare steel specimens that were 0.59 in. thick underwent an average of 8.3 cycles prior to fracture initiation and 13.3 cycles before full fracture. As expected, thicker specimens experienced fracture initiation and propagation in less cycles because the extreme fiber strains were larger for the nominally equal imposed curvature associated with an 11 in. roller. The 0.94 in. thick specimens experienced fracture initiation and full fracture after an average of 2.3 and 4.0 cycles, respectively.

Fracture initiation was observed to occur in many locations across the face of the bare specimens as shown in Figure 3.4a. The cycle associated with fracture initiation was determined visually using six high definition cameras. Upon further bend cycles, the fractures propagated and linked up until one fracture line reached a critical length and the fracture propagated through the rest of the specimen in a sudden and brittle fashion as shown in Figure 3.4b.



Figure 3.4– Fracture initiation at multiple locations at the bottom of Specimen W24-B2-T59-R025 on cycle 3, complete fracture at the bottom side of the specimen at cycle 5.

The 1.0 in. radius side notches caused fracture initiation and final fracture at cycles that were approximately 28% of the cycle number for un-notched specimens. The sharper 0.25” radius notches reduced the number of cycles to fracture initiation and final fracture to approximately 19%

of the un-notched specimens. The side notches increased the stress triaxiality and the plastic equivalent strain as demonstrated in the next section. As discussed in previous chapters, this variation is useful for a more robust calibration of fracture parameters.

Powder Actuated Fastener Specimens (PAF)

The behavior of the powder actuated fastener bend specimens was sensitive to specimen thickness. When the PAF were installed in 0.59 in. thick specimens in the top side of the specimen, the tip of the fastener was close to the surface of the bottom side of the specimen. An observable bump formed on the bottom side as shown in Figure 3.5(a). See Section 2.5 for a definition of the top side and bottom side of a specimen. During cyclic bend testing, fracture initiated at the bump on the back side of the specimen. The fracture propagated relatively slowly compared to other artifacts, and then final fracture through the thickness of the specimen occurred at the location of the PAF tip. The local effect due to the PAF tip was likely the reason that fracture initiated at an average of 2.3 cycles as compared to 8.3 cycles for bare steel specimens. Even though the fracture formed earlier than some other artifact types, the slow fracture propagation led to an average cycle at full fracture of 9.0 as compared to 13.3 average cycles to failure for the bare steel specimens. Although fractures also formed on the top side of the specimen around the head of the PAF, the final fracture occurred when the bottom side of the specimen was in tension.

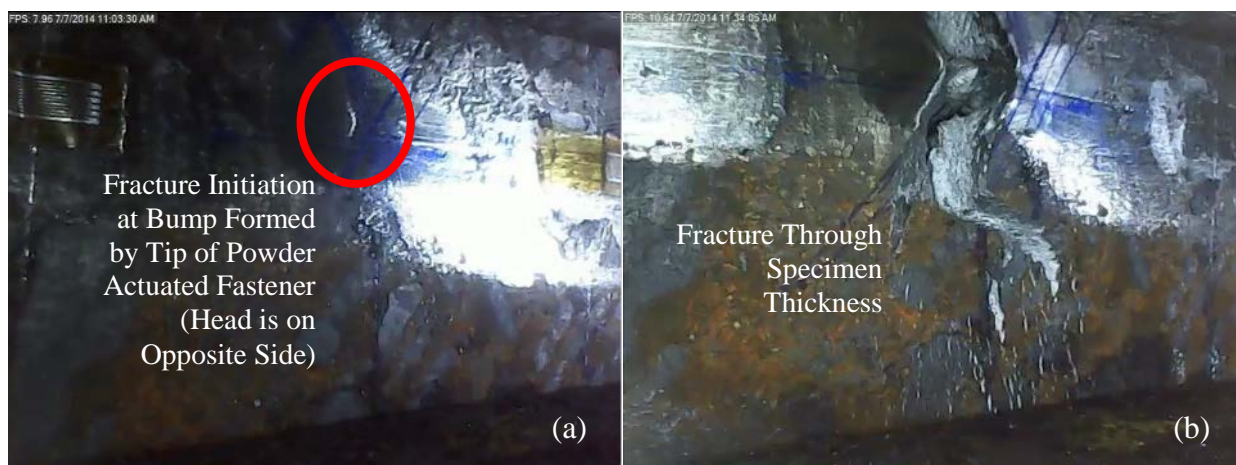


Figure 3.5 – Fracture initiation on Specimen W24-PAF1-T59-R000 at the bottom of the PAF at cycle 3, cycle 18

Thicker specimens with 0.94 in. thickness behaved differently than thinner specimens. Multiple cracks formed in the areas adjacent to the PAF as shown in Figure 3.6. Fracture propagation was observed to happen on the top side around the PAF head until final fracture occurred through the PAF location as shown in Figure 3.6b. For the 0.94 in. thick specimens, the tip of the PAF was more in the center of the specimen closer to the neutral axis. In the absence of local effects described above for thinner specimens, fracture initiation occurred in a similar cycle as the bare specimen. The average cycle at fracture initiation was 2.7 as compared to 2.3 for bare steel specimens. Since 0.94 in. thick specimens with puddle welds had the same average cycle at fracture initiation as PAF, it is likely that the difference in fracture initiation cycle between PAF and bare specimens was due to variability in the material. The cycle at final fracture was 3.7 on average for PAF compared to 4.0 for bare steel specimens. This implies that for the 0.94 in. thick specimens, PAF had little effect on the cycle number when fracture initiated or the cycle when fracture propagated through the specimen.

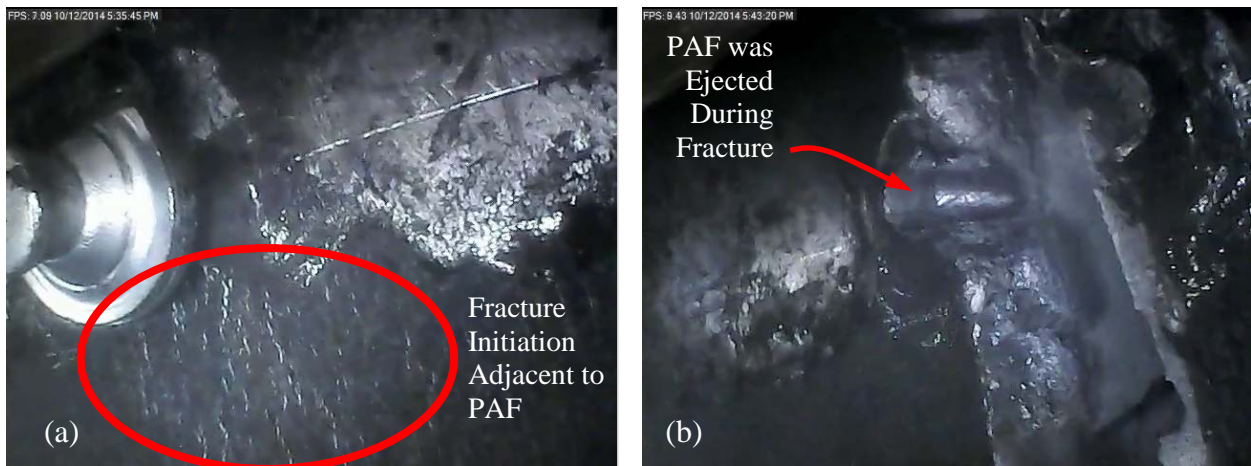


Figure 3.6 – Fracture initiation on Specimen W36-PAF1-T94-R000 at the top of the PAF at cycle 4, complete fracture occurred at the top side of the specimen near the PAF at the beginning of cycle 6.

The following bend test results represent the new testing completed here and are compared to the control specimens of bare steel and powder actuated fasteners from Eatherton and Abbas 2014.

5/8" Pneumatic Actuated Fasteners (PnAF)

Similar to powder actuated fasteners, the effect of the 5/8" PnAF artifacts on the fracture behavior was sensitive to specimen thickness. For all three of the 0.59 in. specimens, fracture was observed to initiate on the top side of the specimen (side with the head of the fastener) near the fastener head as shown in Figure 3.7a. Fracture initiation for all three specimens occurred while the top side with the fastener head was in tension and the bottom side was in compression. The average cycle when fracture initiation occurred was 2.7 compared to 8.3 for the bare steel specimens and 2.3 for the powder actuated fastener specimens. The average cycle at full fracture was 6.3 compared to 13.3 for bare steel specimens and 9 for the powder actuated specimens. For two of the specimens, full fracture occurred on the bottom side when the bottom side was in tension and for one specimen full fracture occurred on the top side when the top side was in tension. Even though the 5/8" PnAF's did slightly better in their fracture initiation cycle, the fracture propagated much faster than in the PAF specimens leading to a final fracture cycle that was much lower. This may have been due to the fact that the fracture initiated on the top of the specimen around the fastener head where the steel was discontinuous due to the fastener shaft rather than on the back side where the continuity of the steel remained intact.

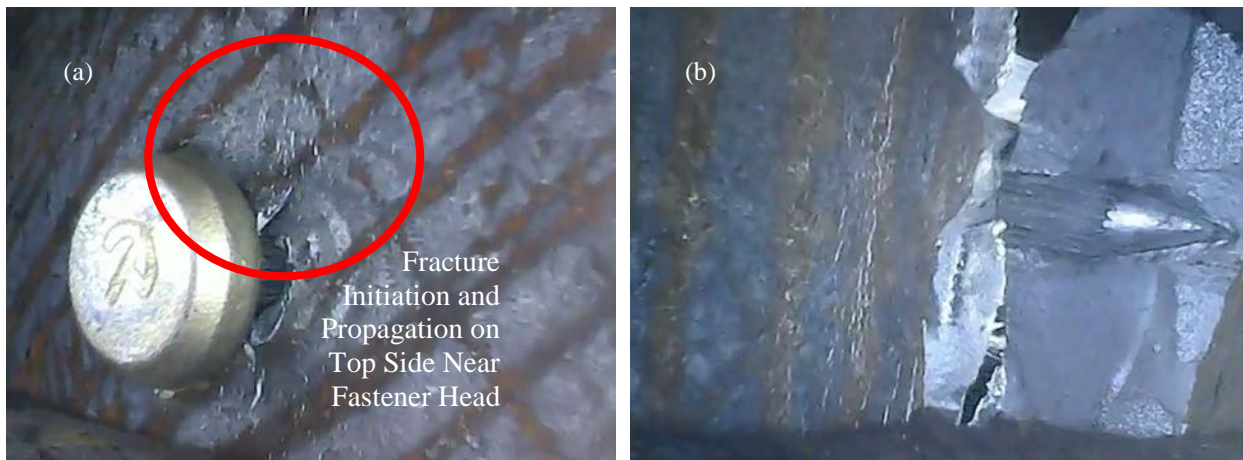


Figure 3.7– (a) Multiple fracture initiation and fracture propagation on Specimen W24-PnAF062.5-T59-R100 at the top and side of the fastener head at cycle 3 while in tension, and (b) complete fracture occurred on Specimen W24-PnAF062.5-T59-R100 at the bottom side of the specimen at cycle 4 while in tension.

In all three of the 0.94 in. thick specimens, fractures also initiated around the fastener head as shown in Figure 3.8a. Fractures initiated and propagated when the top side (side with the fastener head) was in tension. For all three specimens, final fracture through the thickness of the specimen occurred when the fastener head side was in compression (see Figure 3.13b). With an average fracture initiation cycle of 2.3 and average final fracture cycle of 3.3, which are similar to the values for bare steel specimens, however the average final fracture cycle is slightly lower. These are promising results given that the bare steel specimen represents the best case scenario when evaluating defects in the protected zone.

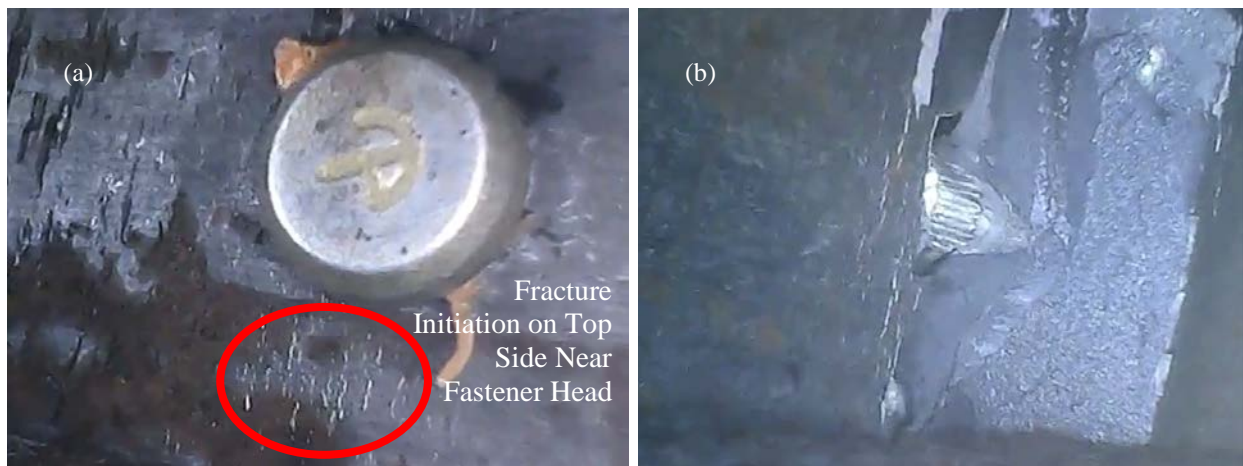


Figure 3.8– (a) Multiple fracture initiation on Specimen W36-PnAF062.5-T94-R025 at the bottom of the fastener head at cycle 2 while in tension, and (b) complete fracture occurred on Specimen W36-PnAF062.5-T94-R025 at the bottom side of the specimen at cycle 2 while in tension.

3/4” Pneumatic Actuated Fasteners (PnAF)

The number of cycles to fracture initiation and propagation for the 3/4” PnAF was also sensitive to specimen thickness although not as sensitive as for the 5/8” PnAF’s. For all three of the 0.59” specimens, fracture was observed to initiate on the top side of the specimen (side with the head of the fastener) near the fastener head as shown in Figure 3.9a. Fracture initiation for all three 0.59” specimens occurred when the top side of the specimen was in tension. Final fracture as seen in Figure 3.9b occurred for all three specimens on the bottom side when the bottom side of the specimen was in tension and the top side was in compression. The average cycle when

fracture initiation occurred was 2.7 compared to 8.3 for the bare steel specimens and 2.3 for the powder actuated fastener specimens. The average cycle at full fracture was 5 compared to 13.3 for bare steel specimens and 9 for the powder actuated fastener specimens.

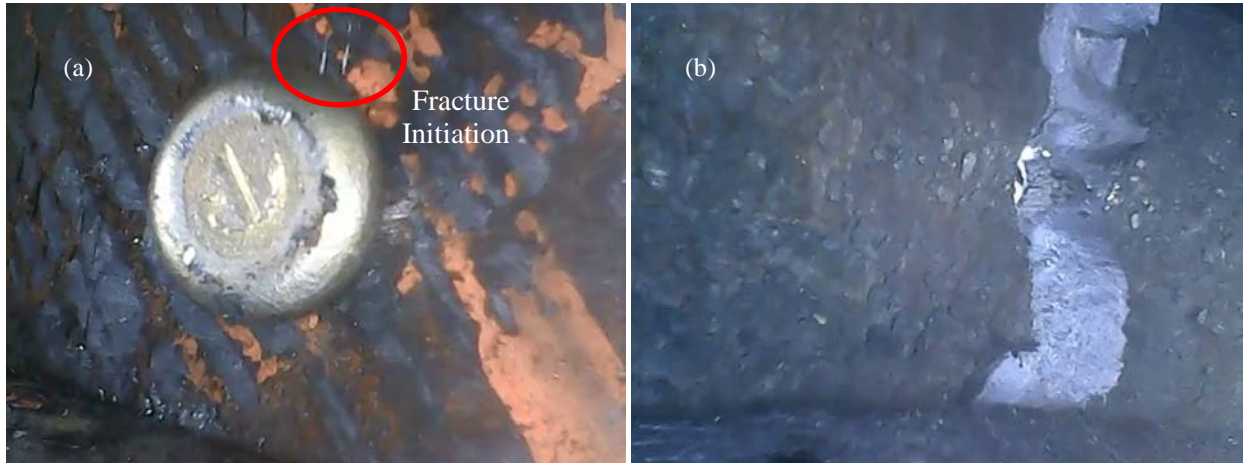


Figure 3.9 – a) Fracture initiation on Specimen W24-PnAF075-T59-R000 on the top side of the specimen near the fastener head at cycle 4 while in tension, and b) Bottom of the specimen showing complete fracture at cycle 9 while in tension.

For the 0.94” thick specimens, fracture was observed to always initiate near the fastener head on the top side of the specimen as shown in Figure 3.10a. Fracture initiation for all of the 0.94” specimens occurred when the top side of the specimen was in tension. For two of the 0.94” thick specimens, final fracture occurred on the bottom side of the specimen when the bottom side was in tension and for one of the 0.94” thick specimens, final fracture occurred on the top side of the specimen when the top side was in tension. The average cycle when fracture initiation occurred was 2 as compared to 2.3 for the bare steel specimens and 2.7 for the powder actuated fastener specimens. The average cycle at full fracture was 3 as compared to 4 for the bare steel specimens and 3.7 for the powder actuated fastener specimens. So in the case of the 3/4” PnAF artifacts, none performed as well as the control in the cyclic tests.

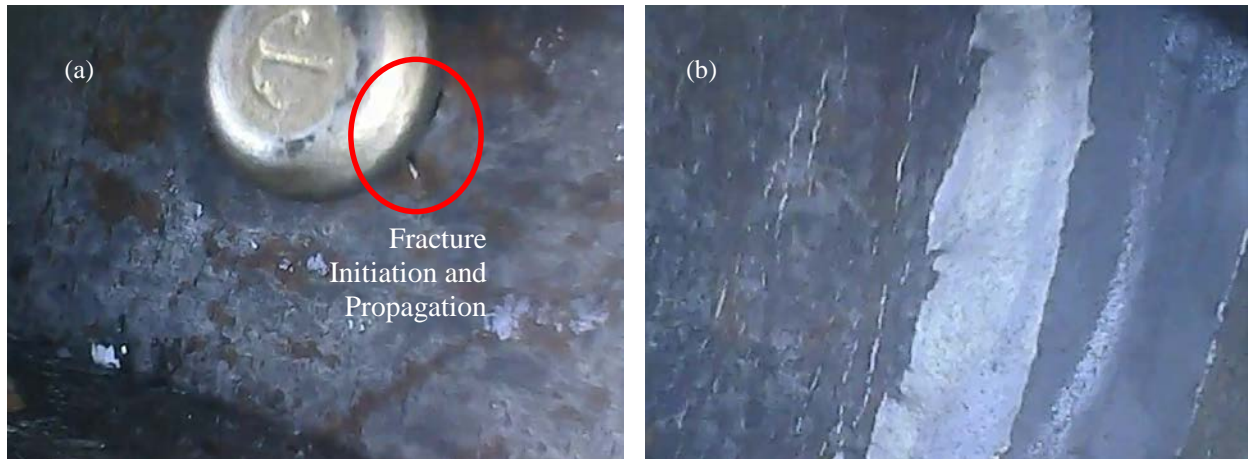


Figure 3.10 – a) Fracture initiation and propagation on Specimen W36-PnAF075-T94-R000 under the fastener head on the top side of the specimen while in tension at cycle 2, and b) complete fracture on back side of specimen while in tension at cycle 5.

Boat Shaped Weld Repair (BSWR)

The fracture initiation for the BSWR specimens was difficult to categorize and was broken up into two categories; cycle of first visible defect and fracture initiation cycle (folded steel defect). The first visible defect describes the very first observed change in the continuity of the steel surface. This usually manifested itself as what looks like a small hole in the weld or, in just one case, typical fracture initiation on the back side of the plate (the side opposite the weld). The fracture initiation cycle (folded steel defect) describes a distinct formation on the weld surface which can be seen in Figure 3.11b. The final full fracture through the specimens always propagated from one of these folded steel defects except in the case where the fracture occurred suddenly before the folded steel defects had a chance to form.

The first visible defect and fracture initiation cycle didn't seem to be effected by specimen thickness however the final fracture cycle was. For the 0.59" specimens, fracture was observed to always initiate and propagate on the top side of the specimen (side with the weld repair) as shown in Figure 3.11a and b. The first visible defect and fracture initiation always occurred when the top of the specimen was in tension. The final fracture for two of the 0.59" thick specimens occurred on the bottom side of the specimen when the bottom side was in tension. For the third 0.59"

specimen, final fracture occurred on the top side of the specimen when the top side was in tension. To compare the results from the BSWR specimen fractures to the bare and PAF control specimens, only the fracture initiation cycle (folded steel defect) and final fracture averages will be considered. This was decided upon because the folded steel defects behaved the most similarly to typical fracture initiation of the two fracture initiation categories. The average cycle when fracture initiation occurred was 2 as compared to 8.3 for the bare steel specimens and 2.3 for the powder actuated fastener specimens. The average cycle at full fracture was 6 as compared to 13.3 for the bare steel specimens and 9 for the powder actuated fastener specimens.



Figure 3.11 – a) First visible defects on specimen W24-BSW-T59-R000 during first cycle on top side of specimen in tension, b) Folded steel defect on specimen during cycle 2 on top side of specimen in tension, and c) final fracture through top side of specimen in tension during cycle 13.

For the 0.94” thick specimens, two had fracture initiation on the top side of the specimen on the weld repair when the top side was in tension, and one had fracture initiation on the bottom side of the specimen (side without the weld repair) when the bottom side was in tension. Typical fracture initiation and propagation on the weld repair can be seen in Figure 3.12. For two of the 0.94” thick specimens, final fracture occurred on the top side of the specimen when the top side was in tension and for one of the 0.94” thick specimens, final fracture occurred on the bottom side of the specimen when the bottom side was in tension. The average cycle when fracture initiation occurred was 2 as compared to 2.3 for the bare steel specimens and 2.7 for the powder actuated fastener specimens. The average cycle at full fracture was 2.7 as compared to 4 for the bare steel specimens and 3.7 for the powder actuated fastener specimens. So for the BSWR artifacts, none of them performed quite as well as the control bare steel or PAF specimens.

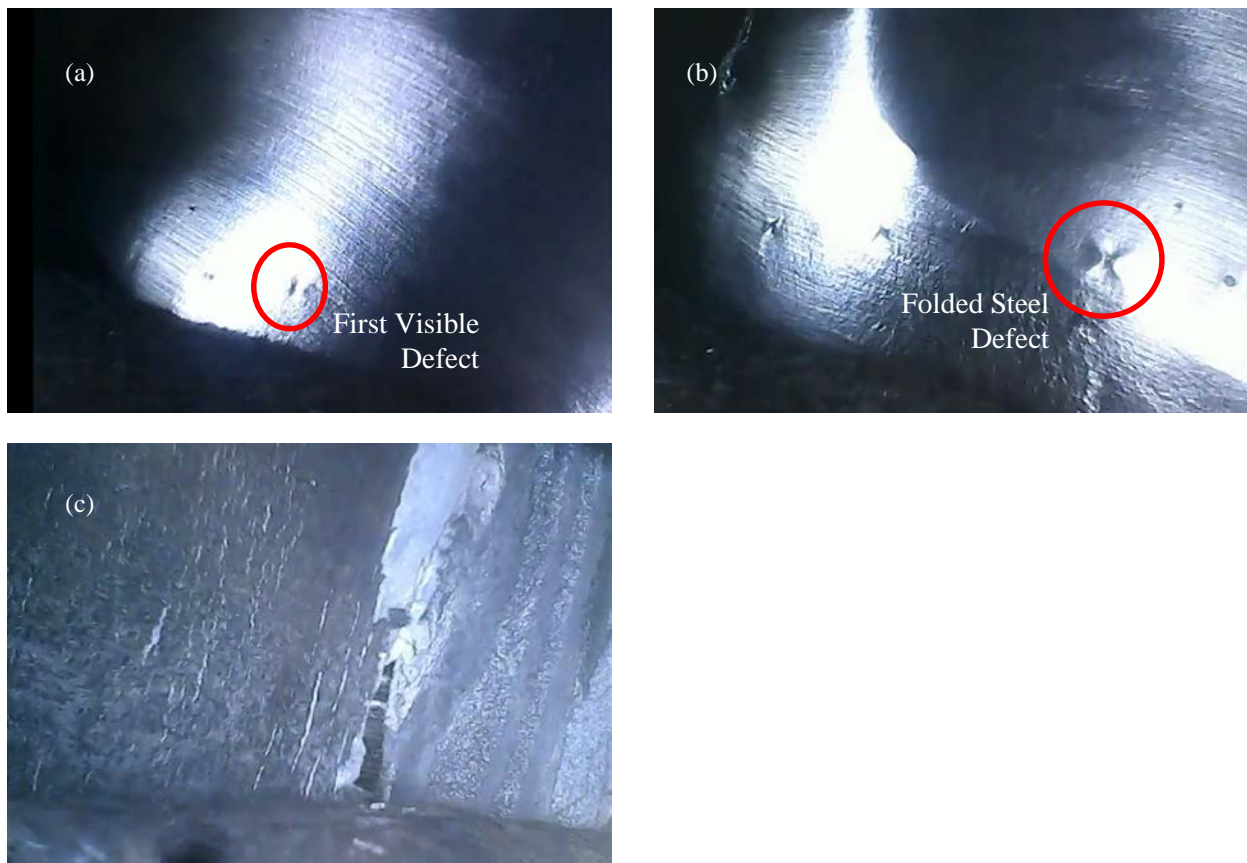


Figure 3.12 – a) First visible defect on specimen W36-BSW-T94-R000 on top side of specimen in tension in the first cycle, b) folded steel defect on top side of specimen in tension in the second cycle, and c) final fracture through bottom side of specimen in tension in cycle 4.

CHAPTER 4 SUMMARY, CONCLUSIONS, AND FURTHER RESEARCH NEEDS

Replicating the monotonic axial tension tests and cyclic bend tests from Eatherton and Abbas (2014), these tests are attempting to demonstrate equivalence to the artifacts known to satisfy SMRF qualifications. Equivalence would be demonstrated by showing that an artifact possesses equal to or better fracture resistance than artifacts known to satisfy SMRF qualifications through full scale testing. To test equivalence, artifacts were compared to the results of two sets of benchmark specimens (bare steel and powder actuated fasteners (PAF)) from Eatherton and Abbas 2014 both known to satisfy SMRF qualifications.

First, cyclic tests were done wherein a flat steel plate is subjected to reverse cyclic inelastic bending. The flat plate specimen is cyclically bent around opposing rollers thus imposing cycles with constant curvature amplitude and therefore constant amplitude of extreme fiber strains. Fracture in seismic structural systems typically occurs at buckling locations that are subjected to large inelastic bending strains. Thus, a cyclic bending test is expected to better capture the strain distribution at critical locations than cyclic axial tests. Then, monotonic axial tension tests were performed where an artifact was installed in a tension coupon with a total length of 18", a gage length of 8", and a width of 1.5". The coupon was then tested using a loading rate conforming to A370-12a (ASTM 2012). The results from the cyclic and monotonic tests were then compared to those from the same tests done on the control specimens from Eatherton and Abbas 2014.

The testing program was applied to specimens with three different artifact types; 0.199" X 5/8" Pneutek pneumatic actuated fasteners (PnAF), 0.199" X 3/4" Pneutek pneumatic actuated fasteners, and boat shaped weld repairs (BSWR). PnAF's represent typical deck attachments or attachment of nonstructural elements to the structural steel beam. The BSWR's are a new type of repair devised for these tests that was thought might be useful for repairing notches, nicks, and gouges in the protected zone of seismic resisting structural systems.

A total of twenty-four cyclic bend tests and monotonic axial tension tests were conducted. Specimens were cut from the flanges of W24x62 (0.59 in. thick) and W36x150 (0.94 in. thick)

beams which were tested previously by Eatherton et al. (2013) in full-scale moment connection tests and are also the same flanges used in Eatherton and Abbas 2014.

Monotonic tests showed that only one artifact performed better than the benchmark PAF artifacts. The average monotonic maximum elongation as a ratio to the powder actuated fastener specimens was 105%, 76%, and 64% for the 5/8" PnAF, 3/4" PnAF, and BSWR respectively. So from the monotonic tests, only the 5/8" PnAF could be argued to have demonstrated equivalence to the benchmark specimens.

Cyclic tests could also be argued to have demonstrated equivalence for the PnAF artifacts when looking at the fracture initiation cycles however the same is not true for the final fracture cycles. As for the BSWR artifacts, they were not close to demonstrating equivalence in any of the cyclic test results. The average number of cycles to fracture initiation were 2.5, 2.3, and 2.0 for the 5/8" PnAF, 3/4" PnAF, and BSWR artifacts respectively. These results can be compared to those from the bare steel and PAF controls which had average fracture initiation cycles of 5.3 and 2.5 respectively. The average number of cycles to full fracture of the specimens were 4.8, 4, and 4.3 for the 5/8" PnAF, 3/4" PnAF, and BSWR artifacts respectively. These are compared to the results from the bare steel and PAF controls which had average final fracture cycles of 8.6 and 6.4 respectively. From the cyclic tests overall, no artifacts performed as well as the controls. The PnAF artifacts came close to demonstrating equivalence to the PAF control but they fell short in the final fracture cycle. This could be explained by the fact that the PnAF artifacts were slightly larger in diameter than the PAF control and thus would be expected to perform slightly worse but could still satisfy the SMRF qualifications. However, it cannot be concluded that any of the artifacts tested do satisfy the SMRS qualifications without full scale testing since none of them definitively demonstrated equivalence to the control.

Another important phenomenon to note is the effect that the specimen thickness had on fracture resistance of an artifact as compared to the bare steel control. The effect of all artifacts on fracture initiation and propagation was found to be sensitive to flange thickness. For instance, PnAF artifacts installed in the 0.94" thick material had very similar fracture initiation cycles as the bare steel control, however the PnAF's installed in the 0.59" thick specimens had vastly lower fracture initiation cycles than the bare steel control. A similar trend was observed for the BSWR specimens. So compared to the bare steel control, the fracture resistance of thicker specimens was

less affected than thinner specimens for all artifacts. However, the thicker specimens resisted less cycles to failure than the thinner specimens and the bare steel control specimen.

The study described herein attempts to determine the likelihood of artifacts meeting the SMRF qualifications by demonstrating equivalence. The study uncovered several challenges associated with the testing methods and results that deserve further research:

1. The 0.199 in. x 0.625 in. pneumatic PAF produced monotonic elongation and number of cycles to fracture initiation and final fracture that were similar or slightly less than benchmark specimens containing powder actuated fasteners. It is not possible, therefore, to conclusively state that these artifacts are acceptable (acceptable defined as likely to satisfy SMRF qualification criteria based on demonstrating equivalence) in the protected zone of special moment resisting frames. However, since the results were not substantially less, it is possible that these artifacts applied in the protected zone would not cause significant fracture before SMRF qualification. To be sure, it would be necessary to conduct full scale moment connection tests to verify.
2. The 0.199 in. x 0.75 in. long pneumatic PAF produced lower monotonic elongation and cycles to fracture. For the thinner material (0.59" thick flange material included in this testing program), the fastener passed all the way through the material and seemed to negatively affect the low cycle fatigue performance. For power (powder or pneumatic) actuated fasteners, it is advisable to limit the length of the fastener to be less than the thickness of the material.
3. The boat-shaped weld repair specimens developed fracture earlier than the pneumatic or powder actuated fastener specimens. More research is required to develop methods to repair defects in the protected zone that don't have such large impact on low cycle fatigue resistance. Some additional boat shaped weld repair specimens are being tested with smaller wire GMAW welding rather than the large diameter wire FCAW welding conducted in this study.

REFERENCES

- ABAQUS. (2012). *Version 6.12*. Providence, RI: Dassault Systèmes Simulia Corp.
- Abbas, E.K., and Eatherton, M.R. (2014). "Test Method For Evaluating The Effect of Artifacts on Seismic Behavior of Moment Frames". *10th U.S. National Conference on Earthquake Engineering*. Anchorage, AK.
- Adey, B. T., Grondin, G. Y., and Cheng, J. J. (2000). "Cyclic Loading of End Plate Moment Connections". *Canadian Journal of Civil Engineering*, Vol. 27, No. 4, pp. 682-701.
- AISC (2010a). (2010). *ANSI/AISC 341-10 Seismic Provisions for Structural Steel Buildings*. Publishes by AISC.
- Anderson, T. L. (2004). *Fracture mechanics: fundamentals and applications*. Boca Raton, FL: CRC Press.
- Armstrong, P. J., and Frederick, C. O. (1966). "*A Mathematical Representation of the Multiaxial Bauschinger Effect*". Berkeley, UK: (No. CEGP Report RD/B/N731). Berkeley Nuclear Laboratories, Research & Development Department.
- ASTM A370-12a. (2012). *A370-12a Standard Test Methods and Definitions for Mechanical Testing of Steel Products*. ASTM.
- ASTM A6/A6M-12. (2012). *A6/A6M-12 Standard Specification for General Requirements for Rolled Structural Steel Bars, Plates, Shapes, and Sheet Piling*.
- AWS D1.8/D1.8M. (2009). *An American National Standard "Structural Welding Code – Seismic Supplement"*. American Welding Society.
- Chi, B., and Uang, C. M. (2002). "Cyclic Response and Design Recommendations of Reduced Beam Section Moment Connections With Deep Columns". *Journal of Structural Engineering*, Vol. 128, No. 4, pp. 464-473.

- Eatherton, M. R., Toellner, B. W., Watkins, C. E., and Abbas, E. (2013). *Experimental Investigation on the Effect of Powder Actuated Fasteners on Seismic Performance of Moment Connections*. Blacksburg, VA: Virginia Tech SEM Report Series. Report No. CE/VPI-ST-13/05.
- Hajjar, J.F., Leon, R.T., Gustafson, M.A., and Shield, C.K. (1998). "Seismic Response of Composite Moment-Resisting Connections. II: Behavior". *ASCE Journal of Structural Engineering*, Vol. 124, No. 8, pp. 877-885.
- Lee, C. H., Jeon, S. W., Kim, J. H., and Uang, C. M. (2005). Effects of Panel Zone Strength and Beam Web Connection Method on Seismic Performance of Reduced Beam Section Steel Moment Connections. *Journal of Structural Engineering*, Vol. 131, No. 12, pp. 1854-1865.
- Lee, M., Kobayashi, G., and Tagawa, Y. (2012). "Comparative Study on Effect of Powder Actuated Nail and Stud Welding on Steel Member". *15 World Conference of Earthquake Engineering, Lisbon 2012*.
- Lemaitre, J., and Chaboche, J.L. (1994). *Mechanics of solid materials*. Cambridge, UK: Cambridge University Press.
- Myers, A. T. (2009). *Testing and Probabilistic Simulation of Ductile Fracture Initiation in Structural Steel Components and Weldments*". Stanford, CA: Stanford University. Report No. 170.
- Rice, J. R., and Tracey, D. M. (1969). "On the Ductile Enlargement of Voids in Triaxial Stress Fields". *Journal of the Mechanics and Physics of Solids*, Vol. 17, No. 3, pp. 201-217.
- Ricles, J. M., Fisher, J. W., Lu, L. -W., & Kaufmann, E. J. (2002). "Development of Improved Welded Moment Connections for Earthquake-Resistant Design". *Journal of Constructional Steel Research*, Vol. 58, 565-604.

APPENDIX A DESCRIPTION OF BEND TEST FRACTURES

The results of the cyclic bend tests are grouped based on the artifact, then specimen thickness and notch radius. See Table 2.2 for specimen names which consist of four numbers. The first number corresponds to the nominal depth of the beam from which the specimen was taken (W24 for W24x62 and W36 for W36x150). The second number is the artifact identification which can take three values (PnAF062.5 = 5/8" pneumatic actuated fastener, PnAF075 = 3/4" pneumatic actuated fastener, BSW = boat shaped weld repair). The third number corresponds to the specimen thickness (T59 for 0.59 in. and T94 for 0.94 in.) and the final number corresponds to the radius of the side notches in the specimen (R000 for no notch, R025 for 0.25 in. radius, R100 for 1.00 in. radius).

A.1 5/8" Pneumatic Actuated Fasteners (PnAF)

A total of six specimens with 5/8" PnAF's were tested (three W24x62 and three W36x150). The W24x62 specimens showed better fracture resistance than the W36x150 specimens for both the notched and un-notched. All of the specimens showed signs of fracture initiation on the top side of the specimen near the fastener head, although final fracture propagation occurred on the bottom side of the specimens in all but one case. Those fracture initiations near the fastener head caused some area loss which weakened the specimen causing the final fracture. Changing the notch size for the W24x62 specimens also had a noticeable effect on the fracture behavior. For the W36x150 notched specimens ($R = 0.25$ and 1.00 in.), both of them exhibited fracture initiation at similar cycles so changing the notch size did not change the fracture behavior for the W36x150 specimens.

Specimen W24-PnAF062.5-T59-R000

The specimen was cycled to 13 cycles before fracture occurred at the center of the specimen. Fracture initiation occurred at the right side of the fastener head during cycle 3. Complete fracture occurred through the top of the specimen while it was in tension at cycle 13. Fracture initiation and final fracture is shown in Figure A.1.

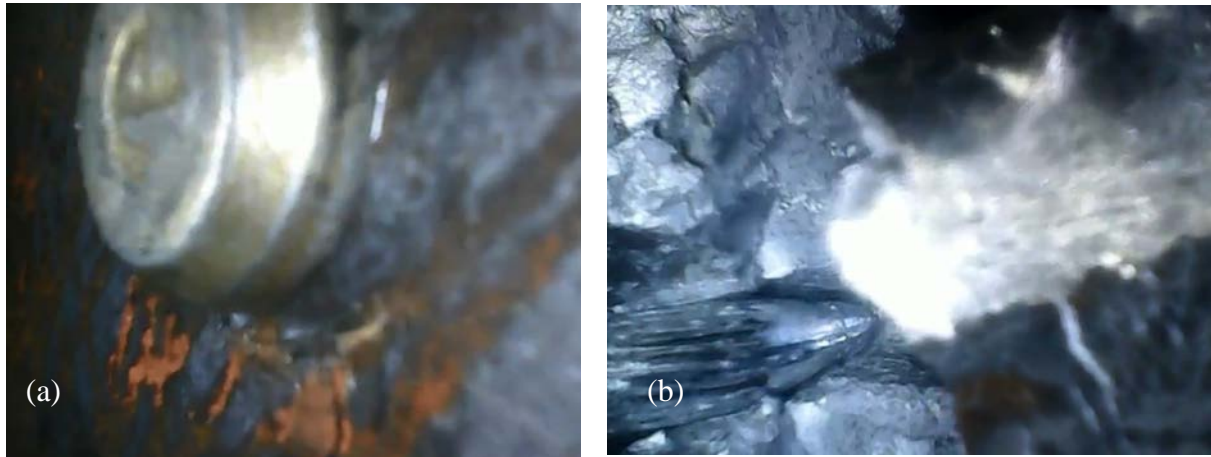


Figure A.1 – (a) Multiple fracture initiation on Specimen W24-PnAF062.5-T59-R000 next to the fastener head while the top side of the specimen was in tension and (b) complete fracture occurred through the top side of the specimen while the top side was in tension.

Specimen W24-PnAF062.5-T59-R025

Fracture initiation was noticed at cycle 2 at the top of the specimen on the right side of the fastener directly under the head as shown in Figure A.2. Full fracture occurred in cycle 2 through the bottom of the plate directly behind the fastener.

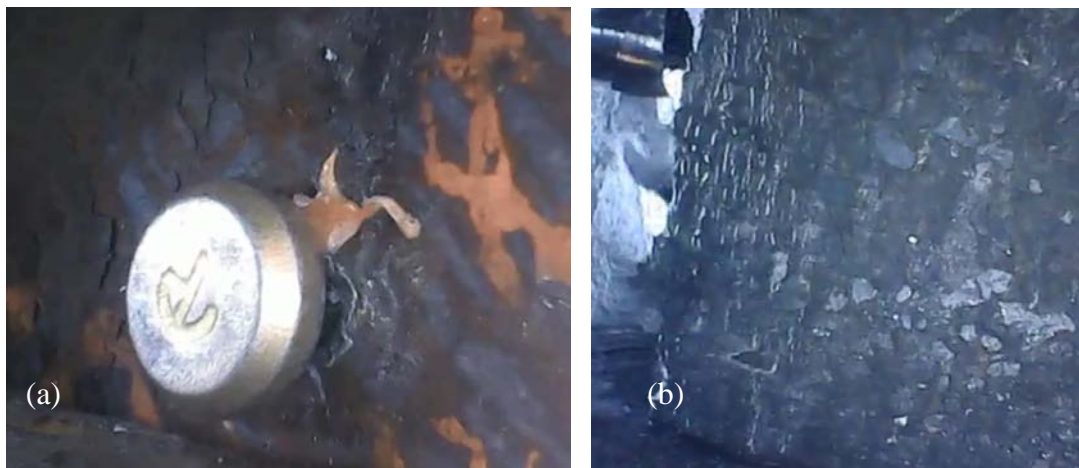


Figure A.2 – (a) Fracture initiation and propagation directly below the fastener head in specimen W24-PnAF062.5-T59-R025 during cycle 2 while the top of the specimen was in tension and (b) Full fracture through the bottom of the specimen during cycle 2 when the bottom was in tension.

Specimen W24-PnAF062.5-T59-R100

Fracture initiation occurred at cycle 3 directly under the head of the fastener as seen in Figure A.3. The fracture propagated at the same location until fracture occurred at cycle 4 through the bottom side of the specimen.

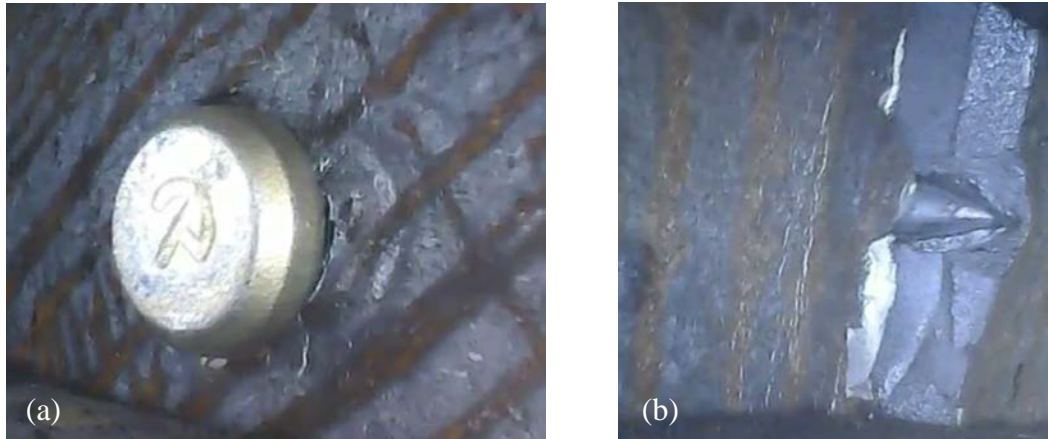


Figure A.1 – (a) Fracture initiation on Specimen W24-PnAF062.5-T59-R100 directly under the fastener head during cycle 3 when the top of the specimen was in tension and (b) full fracture through the back side of the specimen while the back side was in tension.

Specimen W36-PnAF062.5-T94-R000

The specimen was cycled to 2 cycles before fracture occurred next to the fastener head but not right on it. Fracture initiation occurred at multiple locations at the center of the specimen on the top side at cycle 3. Fracture propagated until complete fracture occurred at cycle 5 while the bottom side of the specimen was in tension as shown in Figure A.4. At cycle 3, fracture initiation was noticed at the bottom side of the specimen as shown in Figure A.5.



Figure A.2 – (a) Minor fracture initiation on Specimen W36-PnAF062.5-T94-R000 on the top of the specimen near the head of the fastener and (b) complete fracture occurred at cycle 5 through the bottom side of the specimen.



Figure A.3 – Minor fracture initiation on bottom side of specimen W36-PnAF062.5-T94-R000 during cycle 3 when bottom side was in tension.

Specimen W36-PnAF062.5-T94-R025

Fracture initiation occurred in cycle 2 on the top side of the specimen around the head of the fastener when the top side was in tension as shown in Figure A.6. Fracture propagated quickly and complete fracture occurred also in cycle 2 through the bottom side of the specimen when the bottom side was in tension.



Figure A.4 – a) Multiple fracture initiation on Specimen W36-PnAF062.5-T94-R025 around the fastener head during cycle 2 when the top side of the specimen was in tension and b) full fracture through the bottom side of the specimen when the bottom side was in tension during cycle 2.

Specimen W36-PnAF062.5-T94-R100

Fracture initiation occurred during cycle 2 around the head of the fastener on the top side of the specimen while the top side was in tension and final fracture occurred during cycle 3 on the bottom side of the specimen when the bottom side was in tension. The fracture initiation and final fracture can be seen in Figure A.7. The bottom side also experienced some fracture initiation before full fracture during cycle 2 when the bottom side was in tension as shown in Figure A.8.



Figure A.5 – (a) Fracture initiation and propagation directly under the fastener head in specimen W36-PnAF062.5-T94-R100 during cycle 2 on the top side of the specimen while the top side was in tension and (b) complete fracture through the bottom of the plate during cycle 3 when the bottom was in tension.



Figure A.8 – Fracture initiation on bottom side of specimen during cycle 2 when bottom side was in tension.

A.2 3/4” Pneumatic Actuated Fasteners (PnAF)

A total of six specimens with 3/4” PnAF’s were tested (three W24x62 and three W36x150). The W24x62 specimens showed better fracture resistance than the W36x150 specimens for both the notched and un-notched. Most of the specimens showed signs of fracture initiation around the head of the fastener on the top side of the specimen although final fracture propagation occurred at the bottom side of the specimen in all but one case. Those fracture initiations around the fastener head caused some area loss which weakened the specimen.

Specimen W24-PnAF075-T59-R000

Fracture initiated from the top side of the specimen above the head of the fastener in cycle 4 when the top side was in tension as shown in Figure A.9. Final fracture occurred during cycle 9 through the bottom side of the specimen when the bottom side was in tension. Some fracture initiation was also noticed on the bottom side of the specimen during cycle 6 and can be seen in Figure A.10.



Figure A.9 – (a) Fracture initiation on Specimen W24-PnAF075-T59-R000 at the top of the fastener head during cycle 4 on the top side of the specimen when the top side was in tension and (b) full fracture through the bottom side of the specimen in cycle 9 when the bottom side was in tension.



Figure A.10 –Fracture initiation and propagation through bottom of specimen during cycle 6 when the bottom side was in tension.

Specimen W24-PnAF075-T59-R025

Fracture initiated in cycle 2 around the fastener head on the top side of the specimen when the top side was in tension as seen in Figure A.11. Final fracture also occurred in cycle 2 through the bottom side of the specimen when the bottom side was in tension.

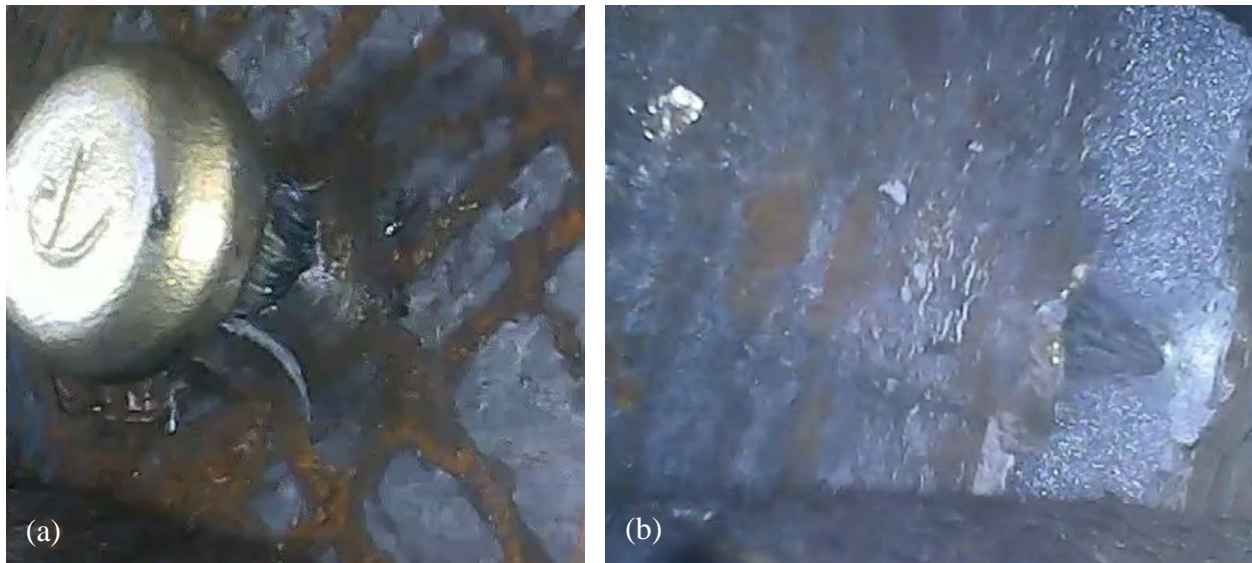


Figure A.11 – (a) Fracture initiation and propagation on specimen W24-PnAF075-T59-R025 right next to the shaft of the fastener during cycle 2 when the top of the specimen was in tension and b) full fracture through the bottom of the specimen during cycle 2 when the bottom of the specimen was in tension.

Specimen W24-PnAF075-T59-R100

Fracture initiated during cycle 2 under the head of the fastener on the top of the shank on the top side of the specimen when the top side was in tension as can be seen in Figure A.12. Full fracture occurred during cycle 4 through the bottom side of the specimen when the bottom side was in tension. Fracture initiation on the bottom side of the specimen was also observed during cycle 3 when the bottom side was in tension. This initiation can be seen in Figure A.13.



Figure A.62 – (a) Fracture initiation on the top side of the fastener shaft during cycle 2 on the top side of the specimen when the top side was in tension and (b) full fracture through the bottom side of the specimen during cycle 4 when the bottom side was in tension.

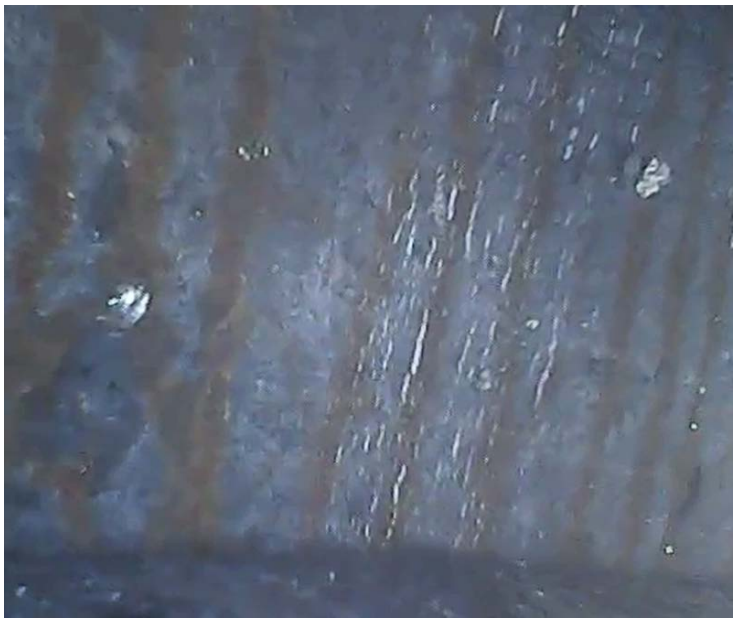


Figure A.13– Fracture initiation on the bottom side of the plate during cycle 3 when the bottom side of the plate was in tension.

Specimen W36-PnAF075-T94-R000

Fracture initiation occurred during cycle 2 around the fastener shaft on the top side of the specimen when the top side was in tension which can be seen in Figure A.14. Final fracture occurred during cycle 5 through the bottom side of the plate when the bottom side was in tension.

It was also observed that fracture initiation occurred on the bottom side of the plate during cycle 3 when the bottom side was in tension. This initiation can be seen in Figure A.15

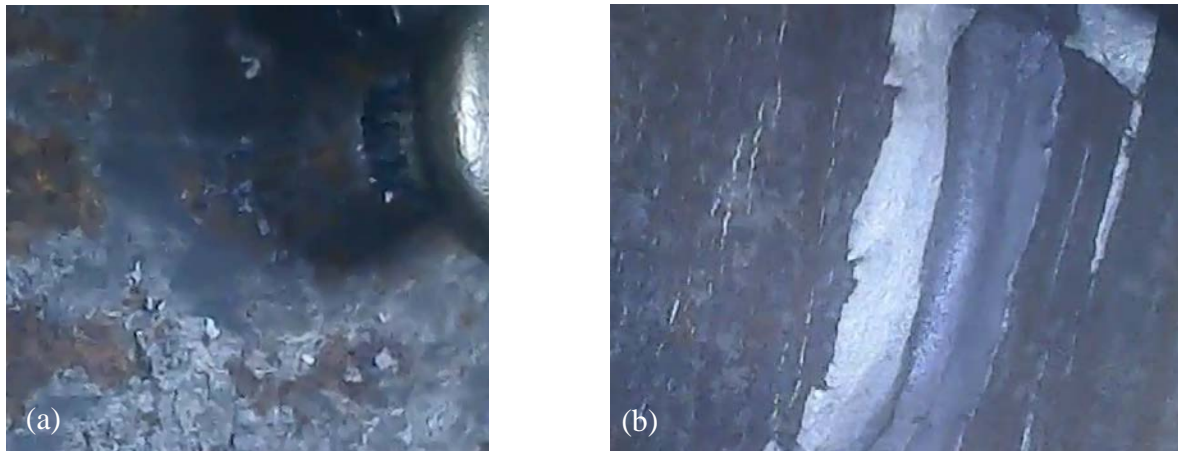


Figure A.14 – (a) Fracture initiation at the very top of the picture by the fastener shaft for specimen W36-PnAF075-T94-R000 occurring at cycle 2 on the top side of the specimen when the top side was in tension and (b) full fracture through the bottom of the specimen during cycle 5 when the bottom side was in tension.



Figure A.15 – Fracture initiation on the bottom side of the plate when the bottom side was in tension during cycle 3.

Specimen W36-PnAF075-T94-R025

Fracture initiation and full fracture both occurred on cycle 2 on the top side of the specimen around the fastener when the top side of the specimen was in tension. This behavior can be seen in Figure A.16.

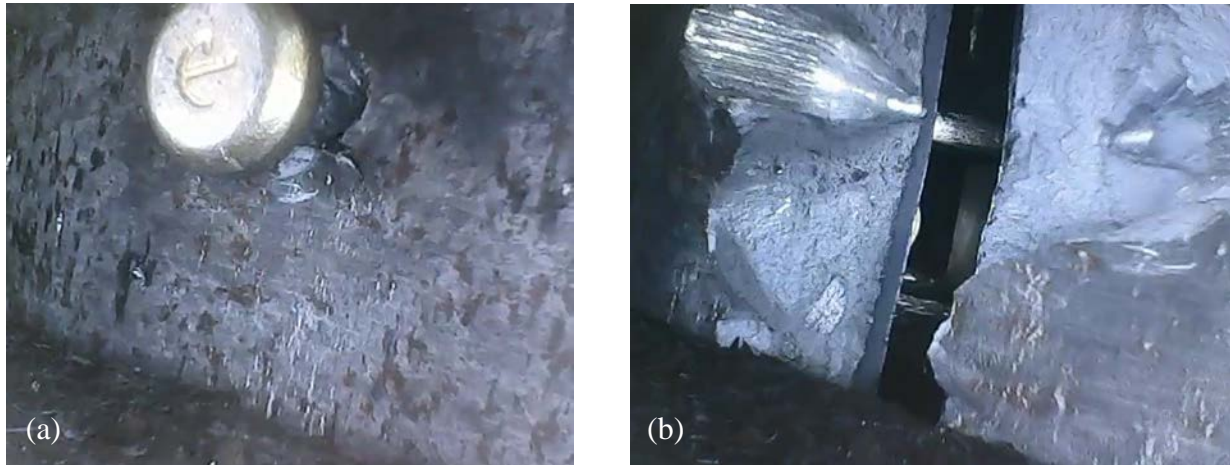


Figure A.16 – (a) Fracture initiation and propagation on specimen W36-PnAF075-T94-R025 around the fastener shaft during cycle 2 when the top side of the specimen was in tension and (b) full fracture through specimen during cycle 2 when the top side of the specimen was in tension.

Specimen W36-PnAF075-T94-R100

Fracture initiated in cycle 2 around the shaft of the fastener on the top side of the specimen when the top side was in tension. Final fracture occurred during cycle 2 through the bottom side of the plate when the bottom side was in tension. This behavior can be seen in Figure A.17.



Figure A.7 – (a) Fracture initiation and propagation during cycle 2 for specimen W36-PnAF075-T94-R100 on the top side of the specimen around the fastener shaft when the top side was in tension and (b) full fracture through the bottom side of the specimen during cycle 2 when the bottom side was in tension.

A.3 Boat Shaped Weld Repair (BSWR)

A total of six specimens with BSWR's were tested (three W24x62 and three W36x150). The grinding was performed using a grinder, for a more detailed process of the BSWR, preparation is explained in chapter 2.

Both of the W24x62 and W36x150 specimens showed poor performance in fracture resistance. All of the specimens showed signs of early fracture initiation and propagation all around the surface of the weld repair. The fracture behavior for these specimens was broken up into three categories; first visible defect, fracture initiation (folded steel defect), and final fracture. See previous chapters for more detailed descriptions of these fracture observations.

Specimen W24-BSW-T59-R000

The first visible defect occurred in cycle 1 and the fracture initiation began in cycle 2 as seen in Figure A.18. Final fracture occurred during cycle 13.

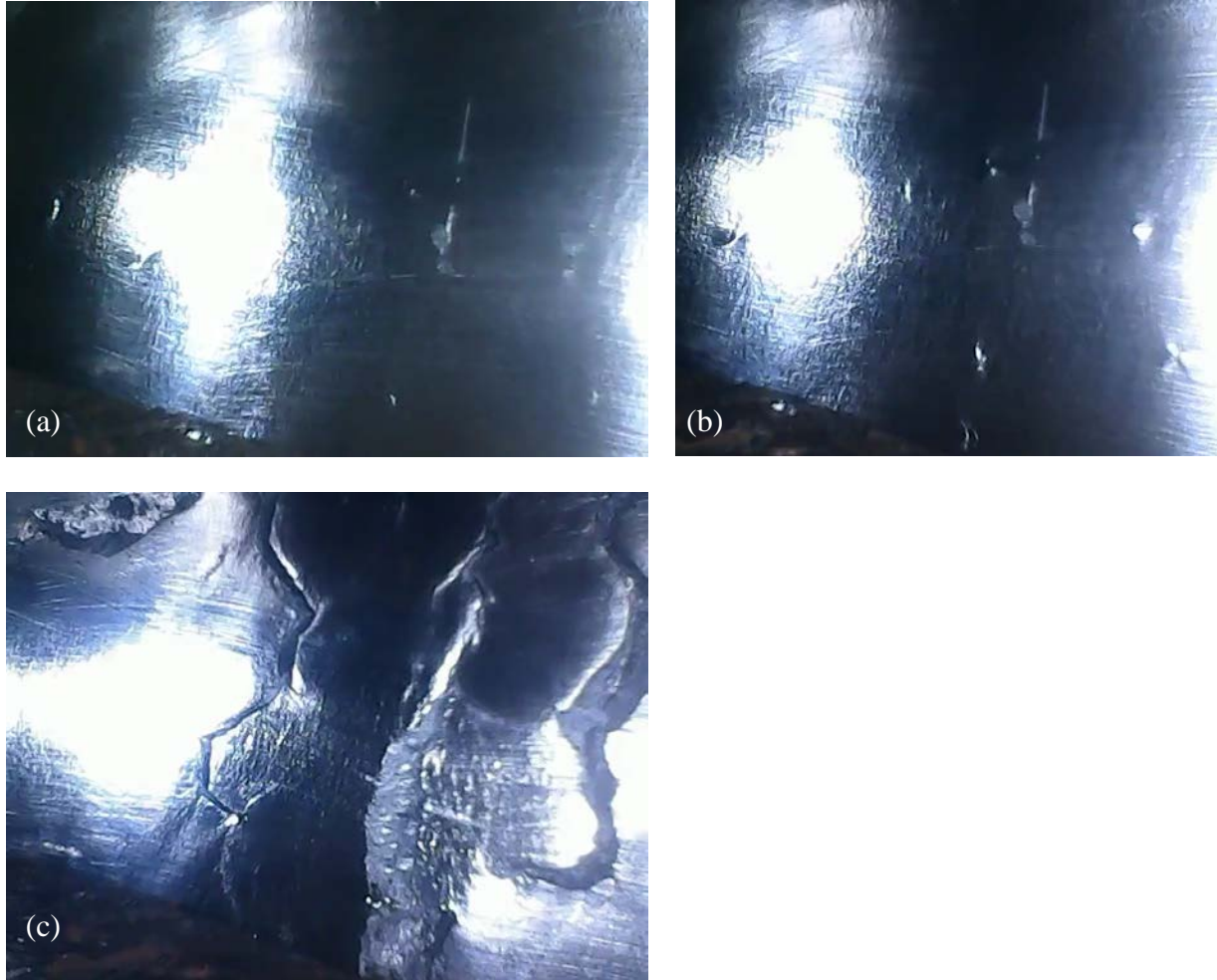


Figure A.8 – (a) Shows first visible defects in specimen W24-BSW-T59-R000 on the surface of the BSWR during cycle 1 when the BSWR is in tension, (b) first folded steel defect can be seen in the bottom right corner after forming during cycle two, and (c) final fracture through top of specimen when the top side was in tension.

Specimen W24-BSW-T59-R025

The first visible defect was observed during cycle 2 on the surface of the weld and final fracture also occurred during cycle 2 through the bottom side of the specimen. Fracture occurred quickly before any folded steel defects had the chance to form. Figure A.19 shows the first visible defects and final fracture.

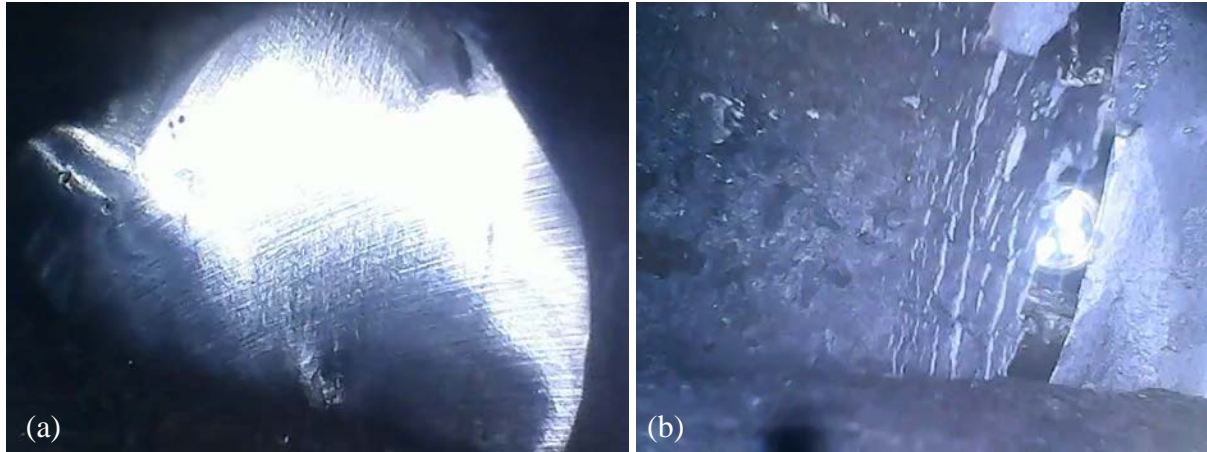


Figure A.19 – (a) First visible defects starting to form on surface of the weld on the top side of specimen W24-BSW-T59-R025 during cycle 2 when the top side was in tension and (b) full fracture through bottom of specimen during cycle 2 when bottom side was in tension.

Specimen W24-BSW-T59-R100

The first visible defect was observed in cycle 1 on the top side of the specimen on the surface of the BSWR, the fracture initiation (folded steel defect) occurred on the surface of the BSWR during cycle 2, and final fracture occurred during cycle 3 through the bottom side of the specimen when the bottom side was in tension. These observations can be seen in Figure A.20



Figure A.90 – (a) First visible defects can be seen around the voids in specimen W24-BSW-T59-R100 during cycle 1, (b) the first folded steel defect can be seen at the bottom of the area with the glare during cycle 2, and (c) full fracture through the bottom of the specimen occurred during cycle 3 when the bottom of the specimen was in tension.

Specimen W36-BSW-T94-R000

The first visible defect occurred during the first cycle on the BSWR surface and the fracture initiation (folded steel defect) occurred on the second cycle also on the BSWR surface. Full fracture occurred on the fourth cycle through the bottom side of the specimen when the bottom side was in tension. These observations can be seen in Figure A.21. Some fracture initiation was also observed on the bottom side of the specimen starting in cycle 3 when the bottom side was in tension. This initiation can be seen in Figure A.22.



Figure A.21 – (a) First visible defects can be seen on weld surface on specimen W36-BSW-T94-R000 during cycle 1, (b) a very clear folded steel defect can be seen in the bottom right of the picture during cycle 2, and (c) full fracture through the bottom side of the specimen in cycle 4 when the bottom side was in tension



Figure A.22 – Fracture initiation on bottom side of specimen during cycle 3 when the bottom side was in tension

Specimen W36-BSW-T94-R025

The first visible defect was observed to occur during the first cycle on the surface of the BSWR and final fracture occurred during the second cycle through the top of the specimen when the top side was in tension. The fracture happened suddenly and no folded steel defects had time to form. Figure A.23 shows the first visible defect and final fracture.

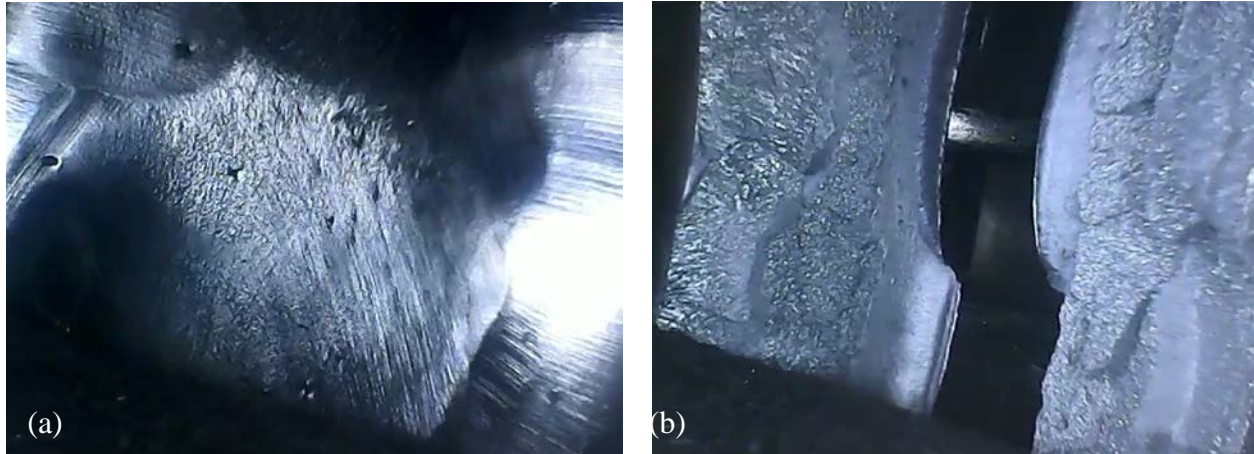


Figure A.23 – (a) First visible defects during cycle 1 on the surface of the BSWR in specimen W36-BSW-T94-R025 and (b) final fracture through the top side of the specimen during cycle 2 when the top side was in tension.

Specimen W36-BSW-T94-R100

The first visible defects were found on the weld surface during cycle 1 when the top of the specimen was in tension. Fracture initiation (folded steel defect) occurred during cycle 2 along with full fracture through the top side of the specimen when the top side was in tension. These observations can be found in Figure A.24.



Figure A.24 – (a) Small visible defects on surface of weld on specimen W36-BSW-T94-R100 during cycle 1, (b) multiple folded steel defects forming in cycle 2 in the area where a void was ground out, and (c) final fracture through top of specimen during cycle 2 when top side was in tension.